Sexually Dimorphic Adolescent Trajectories of Prefrontal Endocannabinoid Synaptic Plasticity Equalize in Adulthood, Reflected by Endocannabinoid System Gene Expression

Axel Bernabeu, Anissa Bara, Michelle Murphy Green, Antonia Manduca, Jim Wager-Miller, Milene Borsoi, Olivier Lassalle, Anne-Laure Pelissier-Alicot, Pascale Chavis, Ken Mackie, et al.

Title

Sexually dimorphic adolescent trajectories of prefrontal endocannabinoid synaptic plasticity equalize in adulthood, reflected by endocannabinoid system gene expression.

Running Title

Sexually dimorphic adolescent trajectories of prefrontal endocannabinoid system

Authors

Axel Bernabeu[1,2,3, #], Anissa Bara[1,2,3, #], Michelle N Murphy Green[3,4 #], Antonia Manduca[1,2,3], Jim Wager-Miller[3,4], Milene Borsoi[1,2,3], Olivier Lassalle[1,2,3], Anne-Laure Pelissier-Alicot[1,2,3,5], Pascale Chavis[1,2,3], Ken Mackie[3,4], Olivier JJ Manzoni[1,2,3,6,*]

Affiliations

[1] INMED, INSERM U1249, Marseille, France.
[2] Aix-Marseille University, France.
[3] Cannalab Cannabinoids Neuroscience Research International Associated Laboratory. INSERM-Aix-Marseille University/Indiana University.
[4] The Gill Center for Biomolecular Science and Department of Psychological and Brain Sciences, Indiana University, Bloomington, Indiana, USA.
[5] APHM, CHU Timone Adultes, Service de Médecine Légale, 13005 Marseille, France.
[6] Lead contact

# These authors have contributed equally to this work.

*Correspondence:
olivier.manzoni@inserm.fr

Keywords: endocannabinoid, prefrontal cortex, postnatal development, sexual dimorphism.

Acknowledgement: portions of this manuscript are available online as a preprint: https://www.biorxiv.org/content/10.1101/2020.10.09.332965v2

Abstract

How sex influences PFC's synaptic development through adolescence remains unclear. Here we describe sex-specific cellular and synaptic trajectories in the rat PFC from adolescence to adulthood. The excitability of PFC layer 5 pyramidal neurons was lower in adult females compared with other developmental stages. The developmental course of endocannabinoid-mediated long-term depression (eCB-LTD) was sexually dimorphic, unlike long-term potentiation or mGluR3-LTD. eCB-LTD was expressed in juvenile females but appeared only at puberty in males. Endovanilloid TRPV1R or eCB receptors were engaged during LTD in a sequential and sexually dimorphic manner. Gene expression of the eCB/vanilloid systems was sequential and sex specific. LTD-incompetent juvenile males had elevated expression levels of the CB1R-interacting inhibitory protein CRIP1a and of the 2AG-degrading enzyme ABHD6. Pharmacological inhibition of ABHD6 or MAGL, enabled LTD in young males, whereas inhibition of AEA's degradation was ineffective. These results reveal sex differences in the maturational trajectories of the rat PFC.

Introduction

The eCB system includes cannabinoid receptors (CB1R and CB2R), the vanilloid receptor TRPV1R, and proteins required for the metabolism, transport, and catabolism of anandamide (AEA) and 2-arachidonoylglycerol (2-AG). The eCB system contributes to CNS development beginning at ontogenesis[1] and continuing throughout the post-natal neurodevelopmental period.[2-8] The eCB system is highly influenced by sex and hormonal regulation.[9,10] For example, in the CNS, circulating levels eCBs and the expression of their major target receptor CB1R, vary with sex and during the phases of the estrous cycle.[11-13] Not surprisingly, human and rodent studies consistently indicate sex differences in the short and long-term effects of cannabis and its components, and the trajectory of cannabis use.[14-19]

The prefrontal cortex (PFC) participates to multiple higher functions such as working memory, reasoning, cognitive flexibility, and emotionally guided behaviors,[20,21] and continues to mature until the end of adolescence. Emerging evidence pinpoints adolescence as a sensitive period of development,[22] described as a postnatal "period of heightened malleability[23] during which external stimuli shape changes in brain structure and function. Illuminating the maturational sequence of the PFC is of particular significance in understanding how sensitive periods contribute to physiological development and the pathological states that have their roots in early life adversity.

During adolescence, the maturation of corticolimbic areas, notably the PFC, implicates the eCB system.[24] The PFC is also a site of dense expression of CB1R[25] and is exquisitely sensitive to various synaptopathies which manifest as a variety of cognitive disease states.[26] Exogenous cannabinoid exposure during the prenatal or the perinatal period results in significant abnormalities in PFC synaptic function, which underlie long-lasting behavioral alterations at adulthood in cannabinoid-exposed rats.[27-30] In spite of substantial evidence that cannabinoid exposure during adolescence affects males and/or females,[15,31-33] the normal maturation profile of the eCB system in the PFC remains obscure.

Here, we applied a cross-sectional strategy to explore the maturational sequence of PFC layer 5 (L5) pyramidal neurons and their excitatory inputs in male and female rats. We report period and sex specific differences in the development and the proteins involved in eCB-mediated long-term depression (LTD) in the rat PFC. In contrast, at the same PFC excitatory synapses, neither long-term potentiation (LTP) nor type II mGluR-LTD varied during adolescent maturation in either sex. These differences were not apparent in the nucleus accumbens, a cognate structure of the mesocorticolimbic system. The intrinsic properties of L5 pyramidal cells also displayed a degree of sex-specific maturation while basic synaptic properties were invariant.

These data support the idea that the eCB system plays a key role in brain sex differences established in adolescence.

Material and Methods

Further information and requests for resources should be directed to the Lead Contact, Olivier J.J. Manzoni (olivier.manzoni@inserm.fr).

Animals

Animals were treated in compliance with the European Communities Council Directive (86/609/EEC) and the United States NIH Guide for the Care and Use of Laboratory Animals. The French Ethical committee authorized the project "Exposition Périnatale aux cannabimimétiques" (APAFIS#18476-2019022510121076 v3). All rats used in France were obtained from Janvier Labs and group-housed with 12h light/dark cycles with ad libitum access to food and water. All groups represent data from a minimum of 2 litters. Female data were collected blind to the estrous cycle. Female and male rats were classified based on the timing of their pubertal maturation. The pubertal period in female rats (approximately postnatal day (P) 28 to P 40) was determined by vaginal opening and first estrus. Balano preputial separation indicated pubertal onset in male rats (around P 40), and sexual maturity is indicated by the presence of mature spermatozoa in the vas deferens, which is achieved around P 60 (Schneider 2008). Thus, the female ages groups were Juvenile 21<P<28; Pubescent 30<P<50 and Adult at P >90. Male groups were: Juvenile 21<P<38; Pubescent 40<P<60 and Adult P >90.

Slice preparation

Adult male and female rats were anesthetized with isoflurane and killed as previously described.[28-31,59] The brain was sliced (300 µm) in the coronal plane with a vibratome (Integraslice, Campden Instruments) in a sucrose-based solution at 4°C (in mM as follows: 87 NaCl, 75 sucrose, 25 glucose, 2.5 KCl, 4 $MgCl_2$, 0.5 $CaCl_2$, 23 $NaHCO_3$ and 1.25 NaH_2PO_4). Immediately after cutting, slices containing the medial prefrontal cortex (PFC) or the nucleus accumbens were stored for 1 hr at 32°C in a low-calcium ACSF that contained (in mm) as follows: 130 NaCl, 11 glucose, 2.5 KCl, 2.4 $MgCl_2$, 1.2 $CaCl_2$, 23 $NaHCO_3$, 1.2 NaH_2PO_4, and were equilibrated with 95% O_2/5% CO_2 and then held at room temperature until the time of recording. During the recording, slices were submerged in the recording chamber and superfused at 2 ml/min with low Ca^{2+} ACSF. All experiments were done at 32°C. The superfusion medium contained picrotoxin (100 µM) to block GABA-A receptors. All drugs were added at the final concentration to the superfusion medium.

Electrophysiology

Whole cell patch-clamp of visualized PFC layer five prelimbic pyramidal neurons and field potential recordings were made in coronal slices containing the PFC or the accumbens as previously described. [28-31,59] Neurons were visualized using an upright microscope with infrared illumination. The intracellular solution was based on K+ gluconate (in mM: 145 K+ gluconate, 3 NaCl, 1 $MgCl_2$, 1 EGTA, 0.3 $CaCl_2$, 2 Na^{2+} ATP, and 0.3 Na^{+} GTP, 0.2 cAMP, buffered with 10 HEPES). The pH was adjusted to 7.2 and osmolality to 290 – 300 mOsm. Electrode resistance was 4 – 6 MOhms.

Whole cell patch-clamp recordings were performed with an Axopatch-200B amplifier as previously described. [28-31,59] Data were low pass filtered at 2kHz, digitized (10 kHz, DigiData 1440A, Axon Instruments), collected using Clampex 10.2 and analyzed using Clampfit 10.2 (all from Molecular Device, Sunnyvale, USA).

Access resistance compensation was not used, and acceptable access resistance was <30 MOhms. The potential reference of the amplifier was adjusted to zero prior to

breaking into the cell. Current-voltage (I-V) curves were made by a series of hyperpolarizing to depolarizing current steps immediately after breaking into the cell. Membrane resistance was estimated from the I-V curve around resting membrane potential (Bara et al. 2018; Borsoi et al. 2019; Scheyer et al. 2019, 2020a, 2020b). Field potential recordings were made in coronal slices containing the mPFC as previously described. [28-31,59] During the recording, slices were placed in the recording chamber and superfused at 2 ml/min with low Ca2+ ACSF. All experiments were done at 32 °C. The superfusion medium contained picrotoxin (100 μM) to block GABA Type A (GABA-A) receptors. All drugs were added at the final concentration to the superfusion medium. The glutamatergic nature of the field EPSP (fEPSP) was systematically confirmed at the end of the experiments using the ionotropic glutamate receptor antagonist CNQX (20 μM), which specifically blocked the synaptic component without altering the non-synaptic component. Both fEPSP area and amplitude were analyzed. Stimulation was performed with a glass electrode filled with ACSF and the stimulus intensity was adjusted ~60% of maximal intensity after performing an input–output curve. Stimulation frequency was set at 0.1 Hz.

Gene expression by qRT-PCR

Wistar rats (founders from Envigo (Indianapolis, IN, USA) and bred in house) were anesthetized, decapitated, and brains were harvested at postnatal days (PND) 25, 46, and 91 and flash frozen in chilled isopentane. The medial prefrontal cortex (mPFC) was isolated using the technique described.[60] RNA purification was conducted using Qiagen's RNeasy Plus Micro Kit (Ref. 74034) and reverse transcription was done using ThermoFisher Scientific's RevertAid First Strand cDNA Synthesis Kit (Ref. K1622) following the manufacturer's instructions. qRT-PCR was performed using Taqman Master Mix (Part No. 4369016) and a combination of probes and primers (Table 1). Samples were run in duplicate and normalized against PND 91 males. Outliers were identified and removed using a ROUT test and statistical significance was established with a one-way ANOVA comparing the means of each group of samples. All procedures were approved by the IU Bloomington Institutional Animal Care and Use Committee.

Data acquisition and analysis

The magnitude of plasticity was calculated at 0-10min and 30–40 min after induction (for TBS-LTP and eCB-LTD) or drug application (mGlu2/3-LTD) as percentage of baseline responses. Statistical analysis of data was performed with Prism (GraphPad Software, San Diego, CA, USA) using tests indicated in the main text after outlier subtraction (Grubb's test, alpha level 0.05). All values are given as mean ±SEM, and statistical significance was set at $p<0.05$.

Results

To establish the postnatal maturational trajectories layer 5 pyramidal PFC synapses, experiments were performed in rats of both sexes, at the juvenile (female 21<P<28; male 21<P<38), pubescent (female 30<P<50; male 40<P<60) and adult stages (P>90 for both sexes)[15].

Sex-specific developmental sequence of retrograde eCB-LTD in the rat PFC

Alterations in one or more categories of PFC synaptic plasticity have been associated with endophenotypes of neuropsychiatric disorders.[34-38] However, most of the above-mentioned studies were performed solely in adult males. A notable exception is the observation that in-utero cannabinoid exposure selectively ablates eCB-LTD in the adult male progeny, while females were spared.[28] Because the PFC and the eCB system both undergo rearrangements during adolescence,[8,15,22] we elected to systematically investigate eCB-LTD in the PFC of juvenile, pubescent and adult rats of both sexes. First, we confirmed that a 10-minute, 10Hz stimulation of the superficial-layers of the PFC in slices obtained from the adults of both sexes, induces a robust eCB-LTD at layer 5 synapses (Figure 1 A-B).[28,31] This identical protocol likewise elicited LTD in slices obtained from pubescent males and females (Figure 1 C-D).[31] To our surprise, eCB-LTD could not be induced in response to this protocol in the PFC of juvenile males, while juvenile females already expressed full-fledged LTD (Figure 1 E-F, Table 2 and 3).

Prefronto-accumbens glutamatergic circuits modulate reward-related behaviors[39,40] and the eCB-system of the accumbens is, much like that of the PFC, impeded following genetic deficits,[41] environmental insults,[42,43] and cannabinoid exposure.[44,45] As shown in Figure 2, accumbens eCB-LTD was readily induced in males (Figure 2 A-B) and females at all developmental stages (Figure 2 C-D, Table 4). None of the pairwise comparisons reached significance. Taken together, the results favor a degree of regional and sex specificity to the maturational profile of eCB-LTD.

We next looked for functional properties that might correspond to the delayed expression of eCB-LTD in juvenile male rats.

mGluR-LTD and NMDAR-LTP do not follow a sex-specific maturational sequence in the rat PFC

We next determined if the sex-specific maturation of LTD in the PFC was global for all forms of LTD or limited to eCB-LTD. We examined a distinct form of LTD in the rat PFC mediated by type II mGluR (i.e. mGluR2/3).[31,34,46,47] mGlu2/3 LTD and eCB-LTD share common presynaptic mechanisms[45] and thus may display similar sex-specific maturational paths. PFC slices from our various groups were exposed for 10-minutes to the mGlu2/3 agonist, LY379268 (300nM) to induce an mGlu2/3-dependent LTD. As shown before,[31] this drug application elicited a significant LTD at layer 5 synapses in slices obtained from adult (Supplemental Figure 1 A-B) or pubescent (Supplemental Figure 1 C-D) rats of both sexes (Supplemental Figure 1 A-B). Similarly, the 10-minute application effectively elicited LTD in slices obtained from juvenile male and female rats (Supplemental Figure 1 E-F). Thus, despite shared downstream pathways, mGlu2/3-LTD does not follow the sex-specific maturational trajectory of eCB-LTD in the PFC of rats (Table 5 and 6).

Next, we elected to investigate a plasticity known to be altered in the PFC of rodent models of neuropsychiatric disorders,[36-38,48] NMDAR-dependent theta-burst induced long-term potentiation (TBS-LTP). The TBS protocol effectively induced a lasting synaptic potentiation in slices obtained from rats of all age periods and both sexes (Supplemental Figure 2, Table 7 and 8), thereby confirming and extending our previous study.[31] The data indicate that PFC TBS-LTP is already mature at the juvenile stage in rats of both sexes and consistently expressed in pubescents and adults of both sexes.

CB1R are functional across development and independently of sex

CB1R functionality is sensitive to several external factors. For example, nutritional imbalance[42] and cannabinoid exposure[44,45,49] can desensitize CB1R and consequently ablate eCB-LTD. We tested if functional CB1R were present in both sexes at the three developmental stages by comparing full dose-response curves for the CB1 agonist CP55,940 in both sexes and across age groups. The dose response curves showed that the potency and efficacy of presynaptic CB1R were similar at all ages in both sexes (Figure 3). Thus, the lack of LTD in juvenile males cannot be attributed to a mere lack of presynaptic inhibitory CB1R. This pharmacological appraisal is supported by the qRT-PCR data showing similar levels of PFC CB1 mRNA in juveniles males and females (see Figure 8).

Sex-specific maturation of PFC pyramidal cell excitability and basic synaptic properties

In search of additional mechanistic insights, we compared intrinsic firing properties of pyramidal neurons in our various experimental groups (Table 9 to 12). Patch-clamp recordings of deep-layer PFC pyramidal neurons were performed in acute PFC slices obtained from juvenile, pubescent, and adult male and female rats. The membrane reaction profiles were measured in response to a series of somatic current steps. Independent of developmental stage or sex all recorded layer 5 PFC neurons showed similar and superimposable *I–V* plots (Figure 4 A-B). Similarly, the resting membrane potential (Figure 4 C-D) and the rheobase (Figure 4 E-F) were alike within and between age and sex groups. Closer examination of the depolarization-driven spikes showed less action potentials in response to somatic current steps in female adults compared to the other developmental stages (Figure 4 G-H). This trait, while suggestive of a lower

excitability of PFC pyramidal neurons in adult females, does not provide a mechanism for the lack of LTD in juvenile male.
Basic synaptic properties were also compared. Input–output profiles were measured in our 6 groups (Table 13 and 14): fEPSPs evoked by electrical stimulation showed a consistent profile distribution in response to increasing stimulation intensity: "input–output" curves were similar across age and sex (Figure 5 A-C). Likewise, the paired-pulse ratio (PPR), a multifactorial parameter of the presynaptic probability of neurotransmitter release, remained unchanged in the experimental groups (Figure 5 D-E, Table 15 and 16). When testing whether the PPR changed throughout development, we observed that paired stimuli elicited with intervals >150ms induced equivalent facilitation in juveniles, pubescent, and adults (Figure 5 D-E). Thus, the release probability of excitatory synapses to PFC layer 5 pyramidal neurons, as estimated from the PPR, was stable throughout developmental stages in both sexes.

Sexually dimorphic mechanisms of LTD

In an earlier study, we revealed a previously unknown sexual difference in the mechanism of PFC eCB-LTD at adulthood: LTD is mediated solely by CB1R in males, in striking contrast to females where activation of TRPV1R (but not CB1R) is required to elicit LTD.[28] We reproduced and extended this observation to show that eCB-LTD engages distinct receptors in male and female depending on their developmental stages (Figure 6). In pubescent and adult males, the induction of LTD was blocked by the CB1R antagonist (SR141716A, Figure 6 A-B) but not by the TRPV1R antagonist (AMG 9810, Figure 6 C-D). Thus, regardless of the developmental stage, male eCB-LTD solely depends on CB1R.
In marked contrast, SR141716A could prevent LTD induction in juvenile and pubescent females (Figure 6 E-H). As shown before,[28] LTD was unaffected by the CB1R antagonist but blocked by AMG9810 in adult females (Figure 6 G-H) and we also now report that AMG9810 blocked LTD in juvenile females (Figure 8 G-H). Curiously, female pubescent LTD was not sensitive to AMG9810 (Figure 6 G-H). Thus, female rats require both CB1R and TRPV1R to make eCB-LTD as juveniles, only CB1R during the pubescent stage, and then solely TRPV1R at adulthood.

Stepwise and sex-specific expression of eCB-system genes in the PFC

Throughout early neurodevelopment, specifically during the transition from the juvenile period to adulthood, significant changes occur in the prefrontal cortex.[50,51] To investigate possible underlying mechanisms behind the sex differences in development of eCB-LTD that was discovered using electrophysiology, we used qRT-PCR to analyze several key molecules of the eCB system (Table 1 and 19). There were several sex-specific and developmental differences identified across the molecules studied. Most relevant for the current study and the sexually dimorphic development of eCB-LTD, there was no difference in CB1 receptor mRNA expression levels between juvenile males and females. However, mRNAs for the cannabinoid receptor interacting protein 1a (CRIP1a) a protein that reduces CB1R mediated G-protein-mediated signaling, or the 2-AG catabolic enzyme ABHD6 are expressed significantly more in males compared to females, only in the juveniles (Figure 7). Interestingly, this could suppress eCB-LTD in males relative to females and points to a potential mechanism. Additionally, males express more mRNA for the AEA catabolic enzyme FAAH, than females at both the juvenile and pubescent ages. The former may also contribute to the lack of eCB-LTD seen in juvenile males.

Augmentation of the circulating levels of 2-AG but not AEA uncovers LTD in juvenile male PFC

The current qRT-PCR profiling (Figure 8) and functional data showing that CB1R mediates LTD in pubescent and adult male rats (Figure 6), as well as the realization that inhibitory CB1R are fully functional in juvenile males (Figure 5), open the possibility that enhancing the circulating levels of 2-AG and/or AEA could allow for the induction of eCB-LTD in juvenile males. Thus, PFC slices were incubated (>45 min) in JZL184 (4 μM), a potent inhibitor of monoacyl-glycerol lipase, the main enzyme degrading 2-AG, to increase basal 2-AG levels prior to the 10-minute, 10Hz stimulation. Here, after JZL184 incubation slices obtained from juvenile males were found to exhibit robust, lasting LTD at layer 5 synapses (Figure 8 A-B, Table 20). Of importance, we verified that pre-treatment with SR141716A prevented the ameliorative actions of JZL184 (Figure 8 C), indicating that the "enabled LTD" was mediated by CB1R (Table 20). Additionally, guided by the qRT-PCR, we tested a specific inhibitor of ABHD6 (WWL70, >45 min 10 μM, Marrs et al. 2010, Jung et al. 2012) or an inhibitor of FAAH (URB597, >45 min 2μM, Bara et al. 2018). Inhibition of ABHD6-mediated 2-AG degradation with WWL70 permitted the full expression of LTD in prepubescent male rats (Figure 8 C), confirming that 2-AG is instrumental in eCB-LTD in immature male rats. In marked contrast, inhibiting the degradation of AEA in juvenile males did not uncover eCB-LTD (Figure 8 C), suggesting that AEA does not contribute to LTD in the immature PFC male system.

Discussion

We applied a cross-sectional strategy to show that in L5 synapses of the rat PFC, the maturation of excitatory input and eCB-mediated synaptic plasticity follows a sex-specific trajectory throughout the juvenile to adult stages. Specifically, we show that while eCB-mediated LTD is already apparent in juvenile females, it is expressed only after the onset of puberty in males. The age-related and sex-specific regulation of eCB plasticity contrasts with other forms of synaptic plasticity examined that were already mature by the initial time of experimental investigation in both sexes.

The intrinsic properties of the major PFC neurons changed little from juvenile to adult age. Features such as resting membrane potentials and rheobase did not vary across age and sex, with the exception that the number of action potentials in response to depolarizing steps was reduced in adult females compared to all other groups, suggesting decreased excitability in the adult females. Like intrinsic membrane properties, two basic synaptic parameters, the paired-pulse ratio, and input-output relationships, were remarkably stable across maturation and sexes. These results suggest that for the most part, cellular and synaptic properties of PFC neurons are established early in life and that the inability to induce eCB-LTD in juvenile males (see below) cannot be attributed to differences in intrinsic properties.

Early life and adolescence are well described periods of changes for the eCB system.[24,52-55] The current data support and extend this concept by showing that a major form synaptic plasticity mediated by eCBs is also subject to developmental regulation and is the substrate of a previously unrecognized sex difference before puberty. Furthermore, the observation that eCB-LTD was consistently expressed in both sexes and at all developmental stages in the accumbens strongly suggests that this sexual dimorphism is specific to the PFC. The PFC achieves maturity late during adolescence and additional work will determine the role of eCB-LTD in the behavioral attributes of adolescence.

Dysfunctional CB1R could underlie the lack of eCB-LTD in juvenile males. Sex differences in CB1R expression start early in life and peak around adolescence.[11,56] Even though CB1R expression peaks with the onset of adolescence[24], our qRT-PCR data showed no difference in CB1R mRNA expression levels between juvenile males and females (Figure 7). The functionality of presynaptic CB1R was evaluated by building dose–response curves for the cannabinoid agonist CP55,940. Maximal inhibitory effects of CP55,940 and its EC50 were comparable in all groups (Figure 3) and like what we previously reported in adult male rats.[28] Thus, one can reasonably exclude the possibility that the lack of PFC eCB-LTD in juvenile males is due to low numbers of or non-functional presynaptic CB1R.

Circulating levels of AEA and 2-AG fluctuate and peak around adolescence.[24,52-55] Here, we used qRT-PCR to show sex-specific and developmental differences in the expression of key molecules of the eCB system. We found that CRIP1a, ABHD6 and FAAH mRNA are expressed significantly more in juvenile males compared to females. It is tempting to hypothesize that this expression profile could hinder the induction of eCB-LTD in males relative to females. Indeed, LTD was fully expressed in when PFC slices from prepubescent male rats were incubated with WWL70 to inhibit ABHD6. In keeping with the idea that 2-AG is instrumental to eCB-LTD in juvenile male rats, we found that inhibiting MAGL uncover LTD in juvenile males. In marked contrast, pharmacological inhibition of FAAH in juvenile males did enable eCB-LTD, showing that AEA does not contribute to LTD at this developmental stage.

Cannabis exposure during adolescence produces multiple long-lasting and sex-specific molecular, synaptic and behavioral alterations.[31-33,55] Based on the current findings it is tempting to attribute at least partially, such differences to underlying sex and state-dependent differences in the maturational window of development during which cannabinoid exposure takes place. Additional behavioral and molecular investigations as well as extended characterizations of plasticity and synaptic functions in animals of both sexes in other brain regions are necessary to provide a more thorough picture of the extent to which adolescent maturation shapes brain functions in adulthood.

Changes in plasticity in response to cannabis in-utero or during adolescence were selective to mPFC eCB-LTD, as mPFC NMDAR-LTP and mGlu3-LTD were consistently expressed and eCB-LTD was not developmentally regulated in the accumbens. The recent finding of increased hippocampal LTP in prepubertal female rats[57] may seem inconsistent with these results, but the presence (current study) or absence[57] of a GABA blocker during LTP induction and perhaps more importantly, the different brain areas (PFC vs. Hippocampus) likely explain this apparent discrepancy. In addition, we also recently found opposite changes in LTD and LTP in the basolateral rat amygdala in males and females during puberty and adulthood.[58]

Collectively, these data highlight that sex is a major determinant of prolonged central synapse maturation. Finally, we previously showed that the consequences of in-utero cannabinoids are expressed differently in the offspring: LTD and social behaviors were impeded in adult male but spared in female.[28] The current findings advance the interpretation of the in-utero data. Taken together, these two studies support the hypothesis that in-utero exposure to THC from cannabis blocks the gain of function in eCB-LTD normally occurring at puberty in the male PFC.

Acknowledgements: The authors are grateful to the Chavis-Manzoni team members for helpful discussions and to Dr. A.F. Scheyer for critical reading and help with writing the manuscript.

Author contributions:

Axel Bernabeu: Conceptualization, Data curation, Formal analysis, Validation, Writing—review and editing.

Anissa Bara: Conceptualization, Data curation, Formal analysis, Validation, Writing—review and editing.

Michelle N Murphy Green: Conceptualization, Data curation, Formal analysis, Validation, Writing—original draft.

Antonia Manduca: Data curation, Formal analysis, Validation.

Milene Borsoi: Data curation, Formal analysis, Validation.

Olivier Lassale: Data curation, Formal analysis, Validation, Methodology.

Anne-Laure Pelissier-Alicot: Conceptualization, Supervision, Funding acquisition, Writing: review and editing.

Pascale Chavis: Conceptualization, Supervision, Project administration, Methodology, Writing: review and editing.

Ken Mackie: Conceptualization, Supervision, Funding acquisition, Methodology, Writing—review and editing

Olivier JJ Manzoni: Conceptualization, Supervision, Funding acquisition, Methodology, Project administration, Writing— original draft, review, and editing.

Funding and Disclosures:

This work was supported by the Institut National de la Santé et de la Recherche Médicale (INSERM); Fondation pour la Recherche Médicale (Equipe FRM 2015 to O.M.) and the NIH (R01DA043982 to K.M and O.M.).

Declarations of interest: The authors declare no competing interests.

References:

1. Hurd YL, Manzoni OJ, Pletnikov MV, et al. Cannabis and the Developing Brain: Insights into Its Long-Lasting Effects. J Neurosci 2019;39(42):8250-8258, doi:10.1523/JNEUROSCI.1165-19.2019
2. Harkany T, Guzman M, Galve-Roperh I, et al. The emerging functions of endocannabinoid signaling during CNS development. Trends Pharmacol Sci 2007;28(2):83-92, doi:10.1016/j.tips.2006.12.004
3. Harkany T, Mackie K, Doherty P. Wiring and firing neuronal networks: endocannabinoids take center stage. Curr Opin Neurobiol 2008;18(3):338-45, doi:10.1016/j.conb.2008.08.007
4. Fride E. Multiple roles for the endocannabinoid system during the earliest stages of life: pre- and postnatal development. J Neuroendocrinol 2008;20 Suppl 1(75-81, doi:10.1111/j.1365-2826.2008.01670.x
5. Jutras-Aswad D, DiNieri JA, Harkany T, et al. Neurobiological consequences of maternal cannabis on human fetal development and its neuropsychiatric outcome. Eur Arch Psychiatry Clin Neurosci 2009;259(7):395-412, doi:10.1007/s00406-009-0027-z
6. Galve-Roperh I, Chiurchiu V, Diaz-Alonso J, et al. Cannabinoid receptor signaling in progenitor/stem cell proliferation and differentiation. Prog Lipid Res 2013;52(4):633-50, doi:10.1016/j.plipres.2013.05.004
7. Lu HC, Mackie K. Review of the Endocannabinoid System. Biol Psychiatry Cogn Neurosci Neuroimaging 2021;6(6):607-615, doi:10.1016/j.bpsc.2020.07.016
8. Bossong MG, Niesink RJ. Adolescent brain maturation, the endogenous cannabinoid system and the neurobiology of cannabis-induced schizophrenia. Prog Neurobiol 2010;92(3):370-85, doi:10.1016/j.pneurobio.2010.06.010
9. Cooper ZD, Craft RM. Sex-Dependent Effects of Cannabis and Cannabinoids: A Translational Perspective. Neuropsychopharmacology 2018;43(1):34-51, doi:10.1038/npp.2017.140
10. Krebs-Kraft DL, Hill MN, Hillard CJ, et al. Sex difference in cell proliferation in developing rat amygdala mediated by endocannabinoids has implications for social behavior. Proc Natl Acad Sci U S A 2010;107(47):20535-40, doi:10.1073/pnas.1005003107
11. Rodriguez de Fonseca F, Cebeira M, Ramos JA, et al. Cannabinoid receptors in rat brain areas: sexual differences, fluctuations during estrous cycle and changes after gonadectomy and sex steroid replacement. Life Sci 1994;54(3):159-70, doi:10.1016/0024-3205(94)00585-0
12. Gonzalez S, Bisogno T, Wenger T, et al. Sex steroid influence on cannabinoid CB(1) receptor mRNA and endocannabinoid levels in the anterior pituitary gland. Biochem Biophys Res Commun 2000;270(1):260-6, doi:10.1006/bbrc.2000.2406
13. Bradshaw HB, Rimmerman N, Krey JF, et al. Sex and hormonal cycle differences in rat brain levels of pain-related cannabimimetic lipid mediators. Am J Physiol Regul Integr Comp Physiol 2006;291(2):R349-58, doi:10.1152/ajpregu.00933.2005
14. Stinson FS, Ruan WJ, Pickering R, et al. Cannabis use disorders in the USA: prevalence, correlates and co-morbidity. Psychol Med 2006;36(10):1447-60, doi:10.1017/S0033291706008361
15. Schneider M. Puberty as a highly vulnerable developmental period for the consequences of cannabis exposure. Addict Biol 2008;13(2):253-63, doi:10.1111/j.1369-1600.2008.00110.x

16. Schepis TS, Desai RA, Cavallo DA, et al. Gender differences in adolescent marijuana use and associated psychosocial characteristics. J Addict Med 2011;5(1):65-73, doi:10.1097/ADM.0b013e3181d8dc62
17. Craft RM, Marusich JA, Wiley JL. Sex differences in cannabinoid pharmacology: a reflection of differences in the endocannabinoid system? Life Sci 2013;92(8-9):476-81, doi:10.1016/j.lfs.2012.06.009
18. Lubman DI, Cheetham A, Yucel M. Cannabis and adolescent brain development. Pharmacol Ther 2015;148(1-16, doi:10.1016/j.pharmthera.2014.11.009
19. Cuttler C, Mischley LK, Sexton M. Sex Differences in Cannabis Use and Effects: A Cross-Sectional Survey of Cannabis Users. Cannabis Cannabinoid Res 2016;1(1):166-175, doi:10.1089/can.2016.0010
20. Goldman-Rakic PS. Cellular and circuit basis of working memory in prefrontal cortex of nonhuman primates. Prog Brain Res 1990;85(325-35; discussion 335-6, doi:10.1016/s0079-6123(08)62688-6
21. Seamans JK, Floresco SB, Phillips AG. Functional differences between the prelimbic and anterior cingulate regions of the rat prefrontal cortex. Behav Neurosci 1995;109(6):1063-73, doi:10.1037//0735-7044.109.6.1063
22. Fuhrmann D, Knoll LJ, Blakemore SJ. Adolescence as a Sensitive Period of Brain Development. Trends Cogn Sci 2015;19(10):558-566, doi:10.1016/j.tics.2015.07.008
23. Steinberg L, Morris AS. Adolescent development. Annu Rev Psychol 2001;52(83-110, doi:10.1146/annurev.psych.52.1.83
24. Meyer HC, Lee FS, Gee DG. The Role of the Endocannabinoid System and Genetic Variation in Adolescent Brain Development. Neuropsychopharmacology 2018;43(1):21-33, doi:10.1038/npp.2017.143
25. Marsicano G, Lutz B. Expression of the cannabinoid receptor CB1 in distinct neuronal subpopulations in the adult mouse forebrain. Eur J Neurosci 1999;11(12):4213-25, doi:10.1046/j.1460-9568.1999.00847.x
26. Scheyer AF, Martin HGS, Manzoni OJ. The endocannabinoid system in prefrontal synaptopathies. Endocannabinoid and Lipid Mediators in Brain Functions. Springer International Publishing: 2017.
27. Manduca A, Servadio M, Melancia F, et al. Sex-specific behavioural deficits induced at early life by prenatal exposure to the cannabinoid receptor agonist WIN55, 212-2 depend on mGlu5 receptor signalling. Br J Pharmacol 2020;177(2):449-463, doi:10.1111/bph.14879
28. Bara A, Manduca A, Bernabeu A, et al. Sex-dependent effects of in utero cannabinoid exposure on cortical function. Elife 2018;7(doi:10.7554/eLife.36234
29. Scheyer AF, Borsoi M, Wager-Miller J, et al. Cannabinoid Exposure via Lactation in Rats Disrupts Perinatal Programming of the Gamma-Aminobutyric Acid Trajectory and Select Early-Life Behaviors. Biol Psychiatry 2020;87(7):666-677, doi:10.1016/j.biopsych.2019.08.023
30. Scheyer AF, Borsoi M, Pelissier-Alicot AL, et al. Maternal Exposure to the Cannabinoid Agonist WIN 55,12,2 during Lactation Induces Lasting Behavioral and Synaptic Alterations in the Rat Adult Offspring of Both Sexes. eNeuro 2020;7(5), doi:10.1523/ENEURO.0144-20.2020
31. Borsoi M, Manduca A, Bara A, et al. Sex Differences in the Behavioral and Synaptic Consequences of a Single in vivo Exposure to the Synthetic Cannabimimetic WIN55,212-2 at Puberty and Adulthood. Front Behav Neurosci 2019;13(23, doi:10.3389/fnbeh.2019.00023

32. Cass DK, Flores-Barrera E, Thomases DR, et al. CB1 cannabinoid receptor stimulation during adolescence impairs the maturation of GABA function in the adult rat prefrontal cortex. Mol Psychiatry 2014;19(5):536-43, doi:10.1038/mp.2014.14
33. Renard J, Rushlow WJ, Laviolette SR. What Can Rats Tell Us about Adolescent Cannabis Exposure? Insights from Preclinical Research. Can J Psychiatry 2016;61(6):328-34, doi:10.1177/0706743716645288
34. Kasanetz F, Lafourcade M, Deroche-Gamonet V, et al. Prefrontal synaptic markers of cocaine addiction-like behavior in rats. Mol Psychiatry 2013;18(6):729-37, doi:10.1038/mp.2012.59
35. Iafrati J, Orejarena MJ, Lassalle O, et al. Reelin, an extracellular matrix protein linked to early onset psychiatric diseases, drives postnatal development of the prefrontal cortex via GluN2B-NMDARs and the mTOR pathway. Mol Psychiatry 2014;19(4):417-26, doi:10.1038/mp.2013.66
36. Thomazeau A, Lassalle O, Iafrati J, et al. Prefrontal deficits in a murine model overexpressing the down syndrome candidate gene dyrk1a. J Neurosci 2014;34(4):1138-47, doi:10.1523/JNEUROSCI.2852-13.2014
37. Labouesse MA, Lassalle O, Richetto J, et al. Hypervulnerability of the adolescent prefrontal cortex to nutritional stress via reelin deficiency. Mol Psychiatry 2017;22(7):961-971, doi:10.1038/mp.2016.193
38. Manduca A, Bara A, Larrieu T, et al. Amplification of mGlu5-Endocannabinoid Signaling Rescues Behavioral and Synaptic Deficits in a Mouse Model of Adolescent and Adult Dietary Polyunsaturated Fatty Acid Imbalance. J Neurosci 2017;37(29):6851-6868, doi:10.1523/JNEUROSCI.3516-16.2017
39. Floresco SB. The nucleus accumbens: an interface between cognition, emotion, and action. Annu Rev Psychol 2015;66(25-52, doi:10.1146/annurev-psych-010213-115159
40. Mateo Y, Johnson KA, Covey DP, et al. Endocannabinoid Actions on Cortical Terminals Orchestrate Local Modulation of Dopamine Release in the Nucleus Accumbens. Neuron 2017;96(5):1112-1126 e5, doi:10.1016/j.neuron.2017.11.012
41. Jung KM, Sepers M, Henstridge CM, et al. Uncoupling of the endocannabinoid signalling complex in a mouse model of fragile X syndrome. Nat Commun 2012;3(1080, doi:10.1038/ncomms2045
42. Lafourcade M, Larrieu T, Mato S, et al. Nutritional omega-3 deficiency abolishes endocannabinoid-mediated neuronal functions. Nat Neurosci 2011;14(3):345-50, doi:10.1038/nn.2736
43. Bosch-Bouju C, Larrieu T, Linders L, et al. Endocannabinoid-Mediated Plasticity in Nucleus Accumbens Controls Vulnerability to Anxiety after Social Defeat Stress. Cell Rep 2016;16(5):1237-1242, doi:10.1016/j.celrep.2016.06.082
44. Mato S, Chevaleyre V, Robbe D, et al. A single in-vivo exposure to delta 9THC blocks endocannabinoid-mediated synaptic plasticity. Nat Neurosci 2004;7(6):585-6, doi:10.1038/nn1251
45. Mato S, Robbe D, Puente N, et al. Presynaptic homeostatic plasticity rescues long-term depression after chronic Delta 9-tetrahydrocannabinol exposure. J Neurosci 2005;25(50):11619-27, doi:10.1523/JNEUROSCI.2294-05.2005
46. Otani S, Daniel H, Takita M, et al. Long-term depression induced by postsynaptic group II metabotropic glutamate receptors linked to phospholipase C and intracellular calcium rises in rat prefrontal cortex. J Neurosci 2002;22(9):3434-44, doi:20026366
47. Huang CC, Yang PC, Lin HJ, et al. Repeated cocaine administration impairs group II metabotropic glutamate receptor-mediated long-term depression in rat medial

prefrontal cortex. J Neurosci 2007;27(11):2958-68, doi:10.1523/JNEUROSCI.4247-06.2007
48. Iafrati J, Malvache A, Gonzalez Campo C, et al. Multivariate synaptic and behavioral profiling reveals new developmental endophenotypes in the prefrontal cortex. Sci Rep 2016;6(35504, doi:10.1038/srep35504
49. Mikasova L, Groc L, Choquet D, et al. Altered surface trafficking of presynaptic cannabinoid type 1 receptor in and out synaptic terminals parallels receptor desensitization. Proc Natl Acad Sci U S A 2008;105(47):18596-601, doi:10.1073/pnas.0805959105
50. Arain M, Haque M, Johal L, et al. Maturation of the adolescent brain. Neuropsychiatr Dis Treat 2013;9(449-61, doi:10.2147/NDT.S39776
51. Konrad K, Firk C, Uhlhaas PJ. Brain development during adolescence: neuroscientific insights into this developmental period. Dtsch Arztebl Int 2013;110(25):425-31, doi:10.3238/arztebl.2013.0425
52. Ellgren M, Artmann A, Tkalych O, et al. Dynamic changes of the endogenous cannabinoid and opioid mesocorticolimbic systems during adolescence: THC effects. Eur Neuropsychopharmacol 2008;18(11):826-34, doi:10.1016/j.euroneuro.2008.06.009
53. Heng L, Beverley JA, Steiner H, et al. Differential developmental trajectories for CB1 cannabinoid receptor expression in limbic/associative and sensorimotor cortical areas. Synapse 2011;65(4):278-86, doi:10.1002/syn.20844
54. Lee TT, Gorzalka BB. Timing is everything: evidence for a role of corticolimbic endocannabinoids in modulating hypothalamic-pituitary-adrenal axis activity across developmental periods. Neuroscience 2012;204(17-30, doi:10.1016/j.neuroscience.2011.10.006
55. Rubino T, Parolaro D. Sex-dependent vulnerability to cannabis abuse in adolescence. Front Psychiatry 2015;6(56, doi:10.3389/fpsyt.2015.00056
56. Rodriguez de Fonseca F, Ramos JA, Bonnin A, et al. Presence of cannabinoid binding sites in the brain from early postnatal ages. Neuroreport 1993;4(2):135-8, doi:10.1097/00001756-199302000-00005
57. Le AA, Lauterborn JC, Jia Y, et al. Prepubescent female rodents have enhanced hippocampal LTP and learning relative to males, reversing in adulthood as inhibition increases. Nat Neurosci 2022;25(2):180-190, doi:10.1038/s41593-021-01001-5
58. Guily P, Lassalle O, Chavis P, et al. Sex-specific divergent maturational trajectories in the postnatal rat basolateral amygdala. iScience 2022;25(2):103815, doi:10.1016/j.isci.2022.103815
59. Scheyer AF, Borsoi M, Pelissier-Alicot AL, et al. Perinatal THC exposure via lactation induces lasting alterations to social behavior and prefrontal cortex function in rats at adulthood. Neuropsychopharmacology 2020;45(11):1826-1833, doi:10.1038/s41386-020-0716-x
60. Wager-Miller J, Murphy Green M, Shafique H, et al. Collection of Frozen Rodent Brain Regions for Downstream Analyses. J Vis Exp 2020;158), doi:10.3791/60474

Figure Legends

Figure 1: Sex-specific maturational trajectory of eCB-LTD in the rat PFC.
A. A 10-minute, 10Hz field stimulation (arrow) of layer 2/3 cells in the PFC elicited a robust eCB-LTD at deep layer synapses in adult rat of both sexes. Average time-courses of mean fEPSPs in PFC slices prepared from male (white circles, n=19) or female rats (grey circle, n=8). **B.** fEPSP magnitude at baseline (-10 to 0 minutes) and LTD (30-40 minutes post-tetanus) values corresponding to the normalized values in A. Individual experiments (light circles) and group average (bold circles), before and after LTD induction show similar eCB-LTD in the PFC of adult of both sexes. **C.** Average time-courses of mean fEPSPs showing that a 10-minute, 10Hz field stimulation (arrow) of layer 2/3 cells in the PFC elicited a robust eCB-LTD at deep layer synapses in pubescent rats of both sexes (male, white circles, n=10; female, grey circle, n=16). **D.** Individual experiments (light circles) and group average (bold circles), before and after LTD induction show similar PFC eCB-LTD in pubescent rats of both sexes. **E.** Average time-courses of mean fEPSPs showing the induction of a robust eCB-LTD at deep layer synapses of pubescent female but not male pubescent rats (male, white circles, n=10; female, grey circle, n=14). **F.** Individual experiments (light circles) and group average (bold circles), before and after LTD induction in the juvenile male (left) and female (right) PFC. Data represent mean ± SEM. Two tailed paired T-test, Ordinary one-way ANOVA, Tukey multiple comparisons test, *P<0.05.

Figure 2: Similar eCB-LTD in the nucleus accumbens core is expressed similarly at all age groups in both sexes.
A. In male rats, eCB-LTD is induced similarly at accumbens synapses at all age groups in response to the 10-minute, 10Hz field stimulation (arrow) the juvenile to adulthood maturation. Average time-courses of mean fEPSPs in Juveniles (white circles, n=14), Pubescents (orange circles, n=5) and Adults (grey circle, n=5). **B.** Individual experiments (light circles) and group average (bold circles), before (baseline) and after (40min) LTD induction showing similar NAC eCB-LTD in male juvenile, pubescent, and adult stages.
C. In female rats, eCB-LTD is induced similarly at accumbens synapses at all age groups in response to the 10-minute, 10Hz field stimulation (arrow) the juvenile to adulthood maturation. Average time-courses of mean fEPSPs in Juveniles (white circles, n=5), Pubescents (orange circles, n=4) and Adults (grey circle, n=5).
D. Individual experiments (light circles) and group average (bold circles), before (baseline) and after (40min) LTD induction showing similar NAC eCB-LTD in female juvenile, pubescent, and adult stages. Data represent mean ± SEM. Two tailed paired T-test, Two tailed unpaired T-test, Ordinary one-way ANOVA, Tukey multiple comparisons test, *P<0.05.

Figure 3: Inhibitory CB_1R are similarly functional at all developmental stages in both sexes.
A. Dose-response curve for the cannabimimetic CP55,940 in juvenile male (orange symbols, n = 3-4 animals, EC_{50} = 0.079 µM, top value 42.17%, 95% CI for EC_{50} = 0.026 – 0.238) and female rats (black symbols, n = 5-6, EC_{50} = 0.316 µM, top value 33.63%, 95% CI for EC_{50} = 0.08 – 1.245)**. B.** Dose-response curve for the CP55,940 in pubescent male (orange symbols, n = 4-7 animals, EC_{50} = 0.026 µM, top value 34.89%, 95% CI for EC_{50} = 0.006 – 0.204) and female rats (black symbols, n = 4-6,

EC_{50} = 0.082 µM, top value 36.85%, 95% CI for EC_{50} = 0.027 – 0.255). **C.** Dose-response curve for the CP55,940 in adult male (orange symbols, n = 3-5 animals, EC_{50} = 0.253 µM, top value 41.21%, 95% CI for EC_{50} = 0.0813 – 0.7853) and female rats (black symbols, n = 5-6, EC_{50} = 0.122 µM, top value 30.5%, 95% CI for EC_{50} = 0.0296 – 0.504). fEPSP amplitudes were measured 30 min after application of CP55,940. Each point is expressed as the percentage of inhibition of its basal value. Error bars indicate SEM.

Figure 4: Sex-specific maturation of the intrinsic properties of layer 5 PFC pyramidal neurons.
A-B. Comparison of current injection steps of 50pA from -400pA to 100pA revealed no differences in the I-V relationship in layer 5 pyramidal neurons of the PFC of female and male groups at the juvenile (white symbols), pubescent (orange symbols), and adult stages (black symbols). **C-D**. Similarly, no difference was found in resting membrane potentials and **(E-F)** rheobases (i.e., the minimum current injection required to elicit an action potential with 10pA progressive current injections steps from 0-200pA). **G.** In male, the number of evoked action potentials in response to increasing depolarizing current steps from 0-600pA did not differ in PFC pyramidal neurons of male rats during the juvenile to adulthood maturation. **H.** In female however, the number of evoked action potentials in response to increasing depolarizing current steps was lower in adults versus juvenile and pubescent. Data represent mean ± SEM. Scatter dot plot represents one animal. Males (Juvenile n=16; Pubescent n=9; Adult n=9); Females (Juvenile n=9; Pubescent n=6; Adult n=7). n= individual animal. Sidak's multiple comparisons test, *P<0.05.

Figure 5: The basic synaptic properties of mPFC pyramidal are identical at all age groups in both sexes.
A-C. Input–output profile from juvenile (A), pubescent (B) and adult mPFC layer 5 fEPSPs. Averaged fEPSP area measured as a factor of stimulus intensity. **D-E**: Short-term plasticity of fEPSPs estimated by the ratio of paired stimulus-induced fEPSPs normalized to the amplitude of the first response in juvenile (white symbols), pubescent (orange symbols), and adult (grey symbols) male (**D**) or female (**E**) rats showed no modification in PPR ratio curves along late postnatal development. n= individual animal. Sidak's multiple comparisons test.

Figure 6: Sex specific mechanisms of LTD across postnatal development
A-D. In males' PFC, LTD is always mediated by CB_1R. **A.** In pubescent and adult males, a > 45 min pre-incubation with the CB_1R antagonist (SR141716A) prevents the induction of 10Hz LTD (arrow). Average time-courses of mean fEPSPs in PFC slices prepared from SR141716A-treated pubescent (orange circles, n=5) and adult (grey circle, n=5) males. **B.** fEPSP magnitude at baseline (-10 to 0 min) and LTD (30-40 min post-tetanus) values. Individual experiments (light circles) and group average (bold circles) in the PFC of male pubescent and adult rats. **C.** In pubescent and adult males, a > 45 min pre-incubation with the TRPV1R antagonist (AMG9810) had no effect on LTD induction (arrow). Average time-courses of mean fEPSPs in PFC slices prepared from AMG9810 pubescent (orange circles, n=5) and adult (grey circle, n=11) males. **D.** fEPSP magnitude at baseline and LTD values. Individual experiments (light circles) and group average (bold circles) in the PFC of pubescent and adult male rats. **E-H.** In females' PFC, back-and-forth CB_1R and TRPV1R are required for LTD **E.** In juvenile and pubescent female, the CB_1R antagonist prevents LTD induction, while the

same protocol elicited a robust eCB-LTD in adult females. Average time-courses of mean fEPSPs in PFC slices prepared from SR141716A-treated juvenile (white circles, n=5) pubescent (orange circles, n=9) and adult (grey circle, n=6) females. **F.** fEPSP magnitude at baseline and LTD. Individual experiments (light circles) and group average (bold circles) after SR141716A in the PFC of pubescent and adult females.
G. In juvenile and adult but not pubescent females, the TRPV1R antagonist prevented eCB-LTD. Average time-courses of mean fEPSPs in PFC slices prepared from AMG9810-tretaed juvenile (white circles, n=13) pubescent (orange circles, n=7) and adult (grey circle, n=5) females **H.** fEPSP magnitude at baseline and LTD. Individual experiments (light circles) and group average (bold circles) show eCB-LTD after AMG9810 incubation in the PFC of female juvenile, pubescent and adult rats. Data represent mean ± SEM. Two tailed paired T-test, Two tailed unpaired T-test, Ordinary one-way ANOVA, Tukey multiple comparisons test, *P<0.05.

Figure 7: Developmental & sex-specific changes in mRNA levels of key components of the eCB system.
A-E. qRT-PCR analysis of eCB system receptors; **F-H** synthesizing enzymes; **I-K** degrading enzymes, and **L** other relevant molecules. One-way ANOVA. Error bars represent SD. **p<0.01, ***p<0.001, ****p<0.0001

Figure 8: Enhancing 2-AG but not AEA effectively uncovers eCB-LTD in the juvenile male PFC.
A. Averaged time courses of 10Hz field stimulations (arrow) of layer 2/3 cells in the PFC of male juvenile rats. In control medium, this protocol failed to induce eCB-LTD at deep layer synapses. However, following a > 45 min pre-incubation with the MAGL inhibitor, JZL 184 (1µM), the previously ineffective low frequency protocol now induced a robust LTD in male juvenile rats. Average time-courses of mean fEPSPs in PFC slices prepared from JZL 184 treated (grey circles, n=8) or untreated (white circle, n=11) juvenile males. **B.** fEPSP magnitude at baseline (-10 to 0 minutes) and LTD (30-40 minutes post-tetanus) values corresponding to the normalized values in A. Individual experiments (light circles) and group average (bold circles) show eCB-LTD after JZL 184- incubation in the PFC of male juvenile rats. **C.** Bar histograms summarizing the effects of inhibiting eCB degradation in juvenile male PFC. As shown in detail in A, JZL184 (light grey bar, n=4) restores LTD in otherwise incompetent juvenile (white bar, n=10) male PFC slices. CB_1R were necessary for the permissive effect of JZL184 effect on LTD: SR141716A preincubation blocked LTD induction in the presence of JZL184 (dark grey bar, n=5). Blocking ABHD6-mediated 2-AG degradation with WWL70 (10µM, > 45 min pre-incubation) allowed the previously ineffective low frequency protocol to induce a robust LTD in male juvenile rats (stiped bar, n=8). In contrast, a > 45 min pre-incubation with the FAAH inhibitor, URB597, 2µM,) was not permissive for LTD in the PFC of male juvenile rats (black bar, n=9). Data represent mean ± SEM. Mann-Whitney test, *P<0.05

Supplemental Figure 1: mGluR2/3-LTD does not follow a sex-specific maturational sequence in the rat PFC.
A. mGluR-LTD, induced by a 10-min application of 30nM LY379268, produced a significant LTD at deep layer synapses in adult rat of both sexes. Average time-courses of mean fEPSPs in PFC slices prepared from male (white circles, n=6) or female rats (grey circle, n=4). **B.** fEPSP magnitude at baseline (-10 to 0 minutes) and LTD (30-40 minutes post-drug washout) values corresponding to the normalized values in A. Individual experiments (light circles) and group average (bold circles), show similar mGluR2/3-LTD in the PFC of adult of both sexes. **C.** Average time-courses showing mGluR2/3-LTD in the PFC of pubescent rats of both sexes (male, white circles, n=8; female, grey circle, n=5). **D.** Individual experiments (light circles) and group average (bold circles), before and after mGluR2/3-LTD induction in pubescent rats of both sexes. **E.** Average time-courses showing the induction of a robust mGluR2/3-LTD in pubescent male and female rats (male, white circles, n=5; female, grey circle, n=4). **F.** Individual experiments (light circles) and group average (bold circles), before and after mGluR2/3-LTD induction in the juvenile male (left) and female (right) PFC. Data represent mean ± SEM. Two tailed paired T-test, Two tailed unpaired T-test, Ordinary one-way ANOVA, Tukey multiple comparisons test, *P<0.05.

Supplemental Figure 2: LTP does not follow a sex-specific maturational sequence in the rat PFC.
A. In male PFC, LTP (arrow, the theta-burst stimulation protocol consisted of five trains of burst with four pulses at 100 Hz, at 200 ms interval, repeated four times at intervals of 10 s) of layer 2/3 cells in elicited a robust LTP at deep-layer synapses at all age groups. Average time-courses of mean fEPSPs in PFC slices prepared from juvenile (white circles, n=10), pubescent (orange circle, n=7) and adult (grey circle, n=11) male rats. **B.** Individual experiments (light circles) and group average (bold circles), before and after LTP induction show similar LTP at all stages. **C.** In female rats, LTP is induced similarly in juvenile, pubescent, and adult groups. Average time-courses of mean fEPSPs in Juveniles (white circles, n=9), Pubescents (orange circles, n=7) and Adults (grey circle, n=5). **D.** Individual experiments (light circles) and group average (bold circles) show similar LTP in female at all stages. Data represent mean ± SEM. Two tailed paired T-test, Two tailed unpaired T-test, Ordinary one-way ANOVA, Tukey multiple comparisons test, *P<0.05.

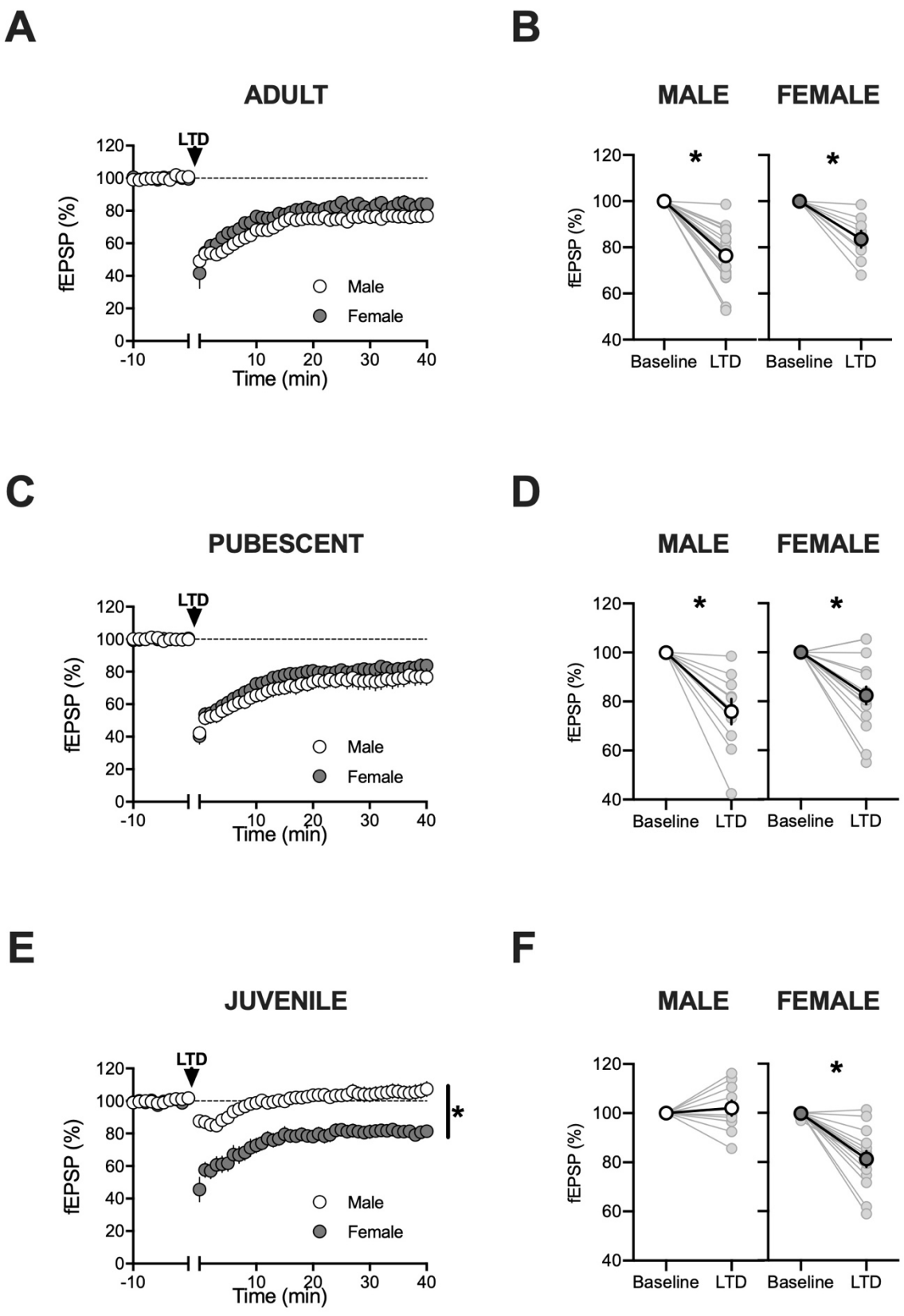
A
ADULT
LTD
fEPSP (%)
Male
Female
Time (min)
B
MALE
FEMALE
fEPSP (%)
Baseline
LTD
C
PUBESCENT
D
E
JUVENILE
F

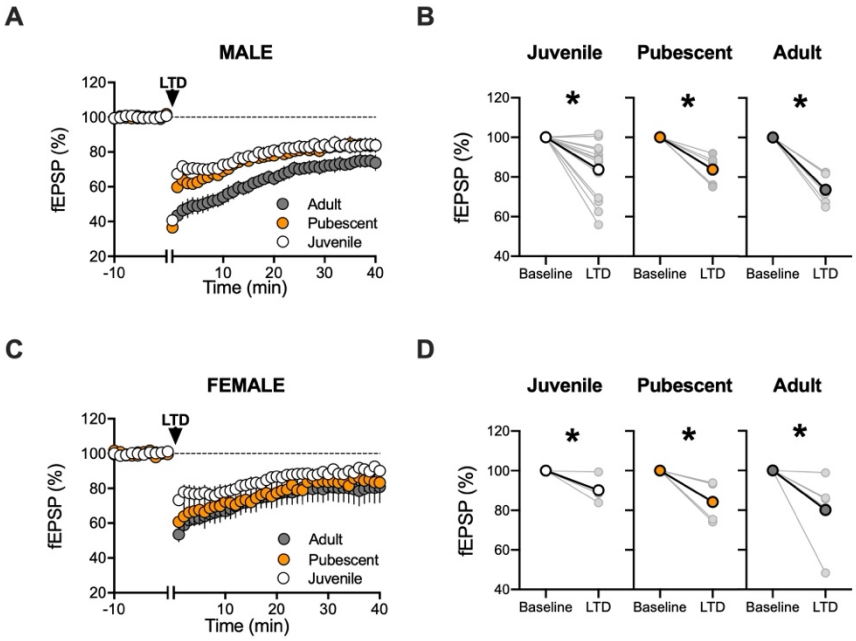
A
MALE
LTD
fEPSP (%)
Time (min)
Adult
Pubescent
Juvenile
B
Juvenile
Pubescent
Adult
fEPSP (%)
Baseline
LTD
C
FEMALE
LTD
fEPSP (%)
Time (min)
Adult
Pubescent
Juvenile
D
Juvenile
Pubescent
Adult
fEPSP (%)
Baseline
LTD

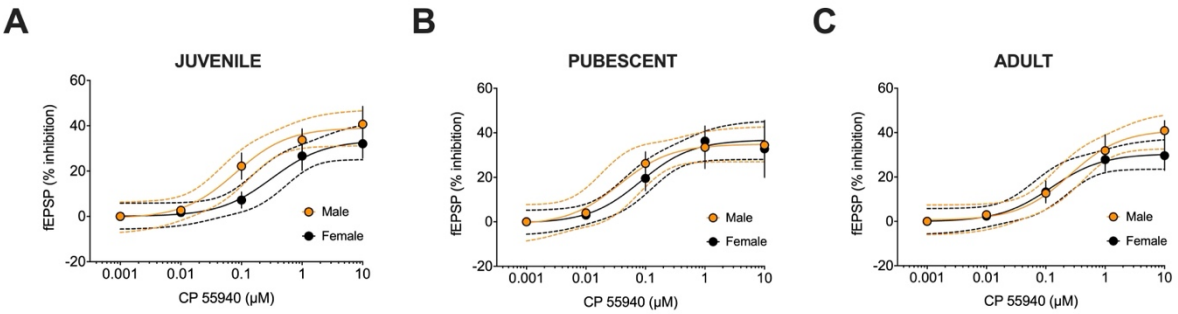
A
JUVENILE
fEPSP (% inhibition)
Male
Female
CP 55940 (μM)
B
PUBESCENT
fEPSP (% inhibition)
Male
Female
CP 55940 (μM)
C
ADULT
fEPSP (% inhibition)
Male
Female
CP 55940 (μM)

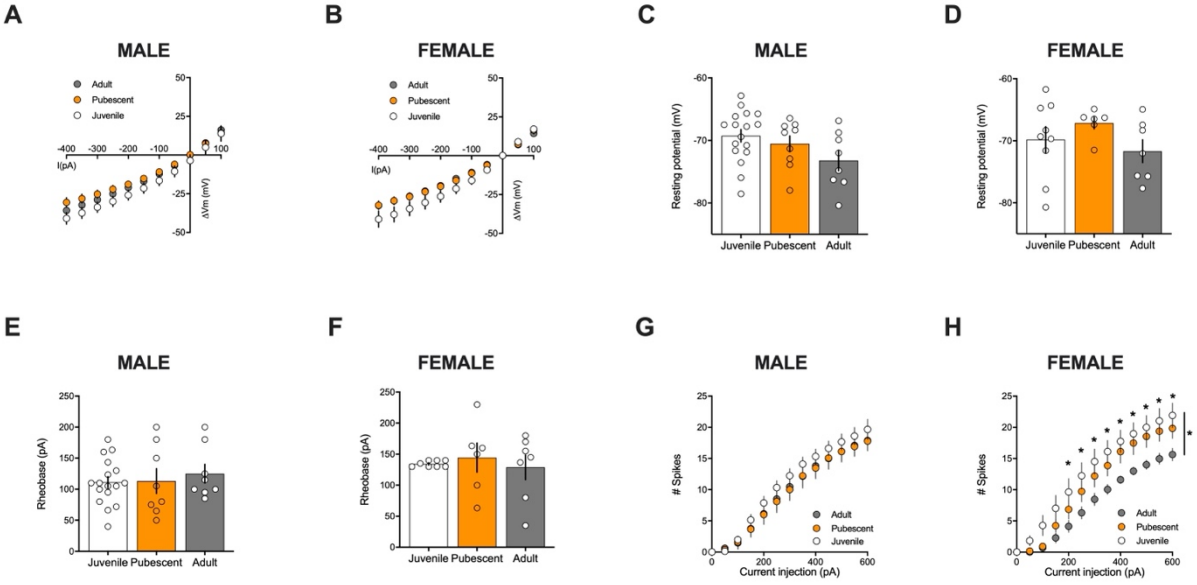
A
MALE
Adult
Pubescent
Juvenile
I(pA)
ΔVm (mV)
B
FEMALE
Adult
Pubescent
Juvenile
I(pA)
ΔVm (mV)
C
MALE
Resting potential (mV)
Juvenile Pubescent Adult
D
FEMALE
Resting potential (mV)
Juvenile Pubescent Adult
E
MALE
Rheobase (pA)
Juvenile Pubescent Adult
F
FEMALE
Rheobase (pA)
Juvenile Pubescent Adult
G
MALE
Spikes
Adult
Pubescent
Juvenile
Current injection (pA)
H
FEMALE
Spikes
Adult
Pubescent
Juvenile
Current injection (pA)

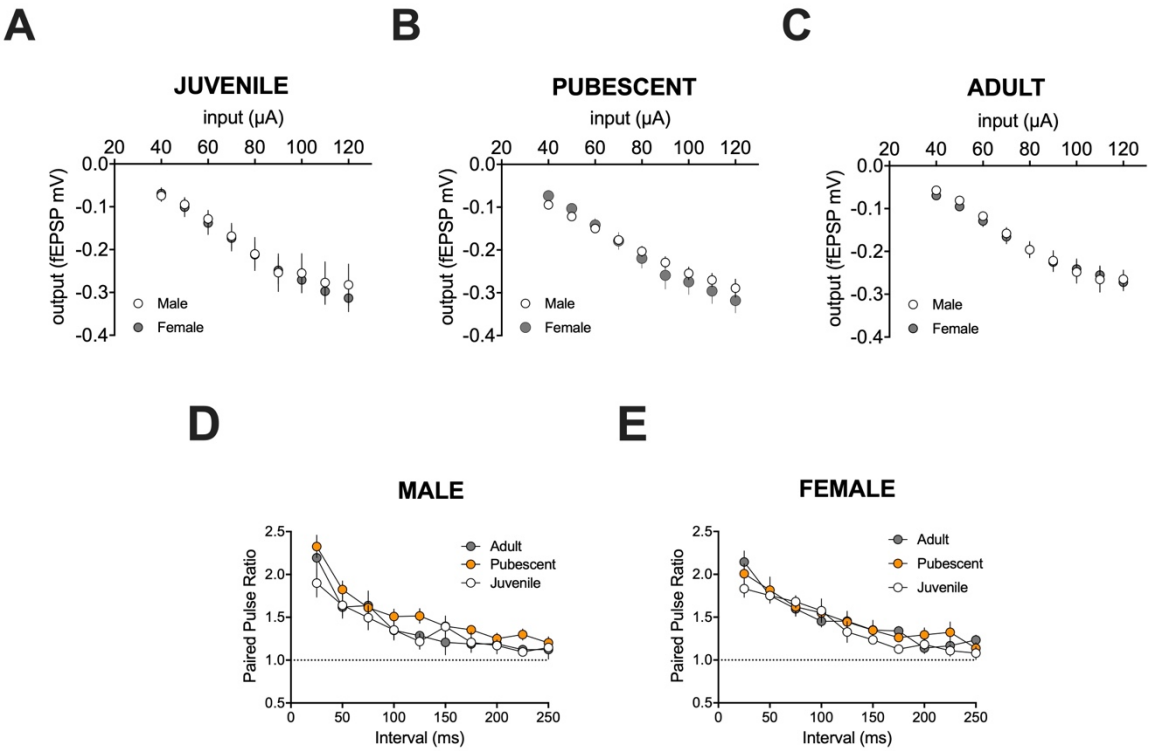
A
JUVENILE
input (μA)
20 40 60 80 100 120
output (fEPSP mV)
0.0 -0.1 -0.2 -0.3 -0.4
Male
Female
B
PUBESCENT
input (μA)
20 40 60 80 100 120
output (fEPSP mV)
0.0 -0.1 -0.2 -0.3 -0.4
Male
Female
C
ADULT
input (μA)
20 40 60 80 100 120
output (fEPSP mV)
0.0 -0.1 -0.2 -0.3 -0.4
Male
Female
D
MALE
Paired Pulse Ratio
2.5 2.0 1.5 1.0 0.5
0 50 100 150 200 250
Interval (ms)
Adult
Pubescent
Juvenile
E
FEMALE
Paired Pulse Ratio
2.5 2.0 1.5 1.0 0.5
0 50 100 150 200 250
Interval (ms)
Adult
Pubescent
Juvenile

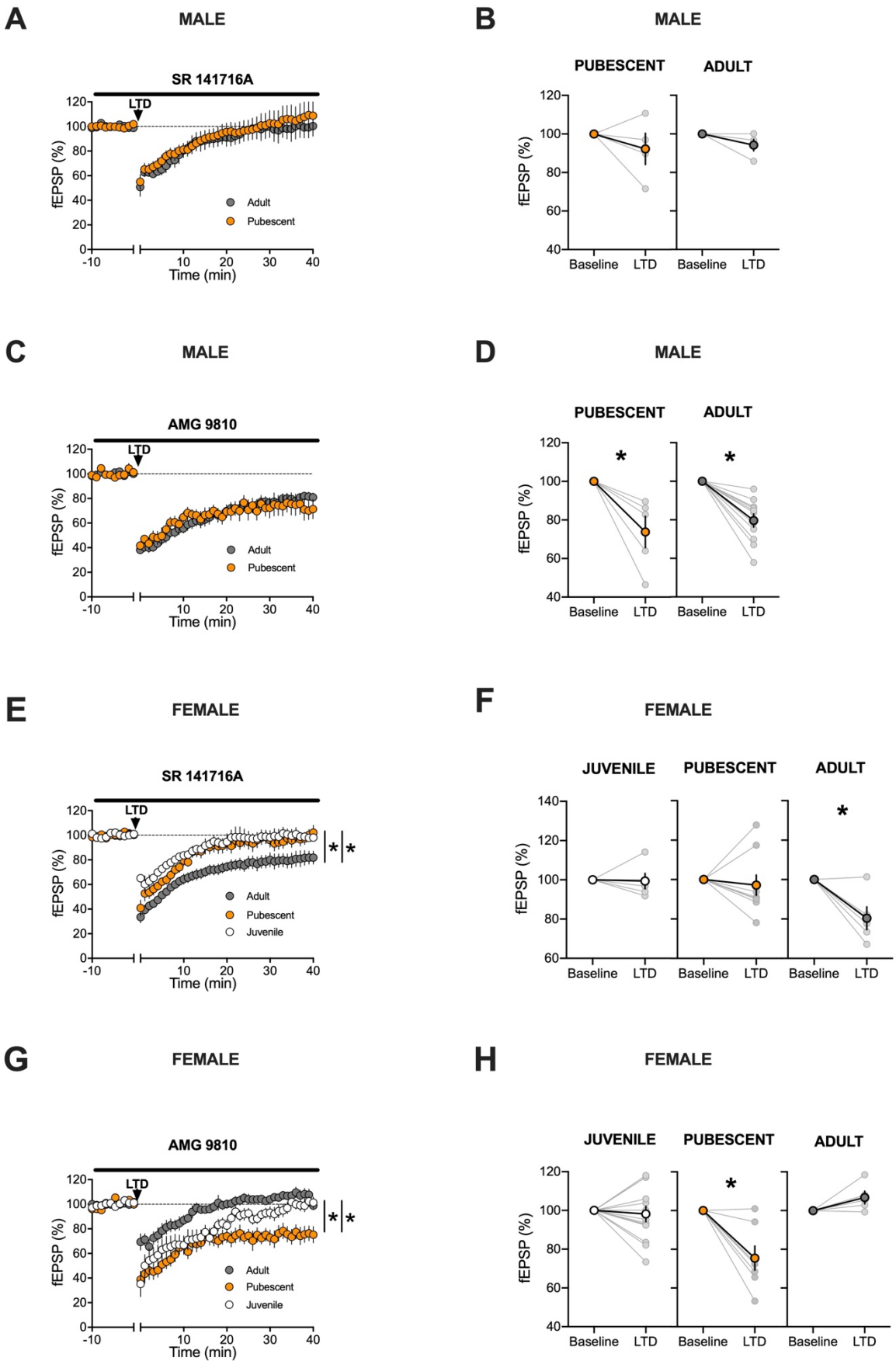
A
MALE
SR 141716A
LTD
fEPSP (%)
Time (min)
Adult
Pubescent
B
MALE
PUBESCENT
ADULT
fEPSP (%)
Baseline
LTD
C
MALE
AMG 9810
LTD
fEPSP (%)
Time (min)
Adult
Pubescent
D
MALE
PUBESCENT
ADULT
*
fEPSP (%)
Baseline
LTD
E
FEMALE
SR 141716A
LTD
fEPSP (%)
Time (min)
Adult
Pubescent
Juvenile
* *
F
FEMALE
JUVENILE
PUBESCENT
ADULT
*
fEPSP (%)
Baseline
LTD
G
FEMALE
AMG 9810
LTD
fEPSP (%)
Time (min)
Adult
Pubescent
Juvenile
* *
H
FEMALE
JUVENILE
PUBESCENT
ADULT
*
fEPSP (%)
Baseline
LTD

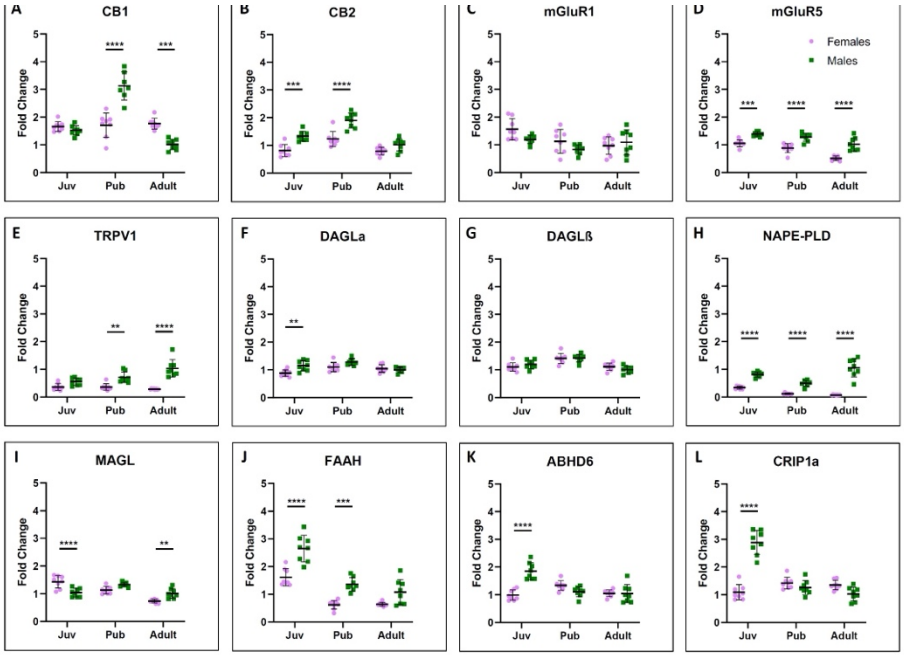
A
CB1
B
CB2
C
mGluR1
D
mGluR5
Females
Males
E
TRPV1
F
DAGLa
G
DAGLß
H
NAPE-PLD
I
MAGL
J
FAAH
K
ABHD6
L
CRIP1a
Fold Change
Juv
Pub
Adult

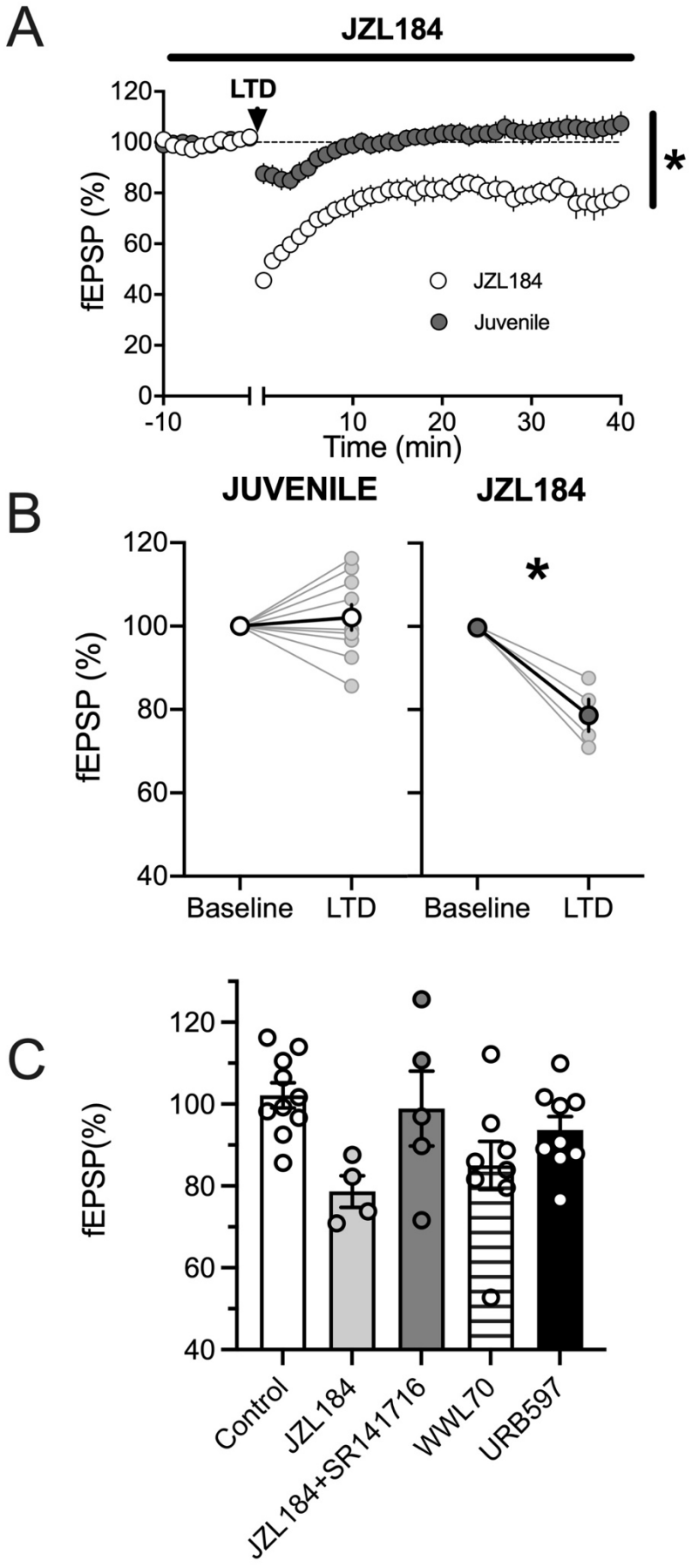
A
JZL184
LTD
120
100
80
60
40
20
0
fEPSP (%)
*
JZL184
Juvenile
-10
10
20
30
40
Time (min)
B
JUVENILE
JZL184
120
100
80
60
40
fEPSP (%)
*
Baseline
LTD
Baseline
LTD
C
120
100
80
60
40
fEPSP(%)
Control
JZL184
JZL184+SR141716
WWL70
URB597

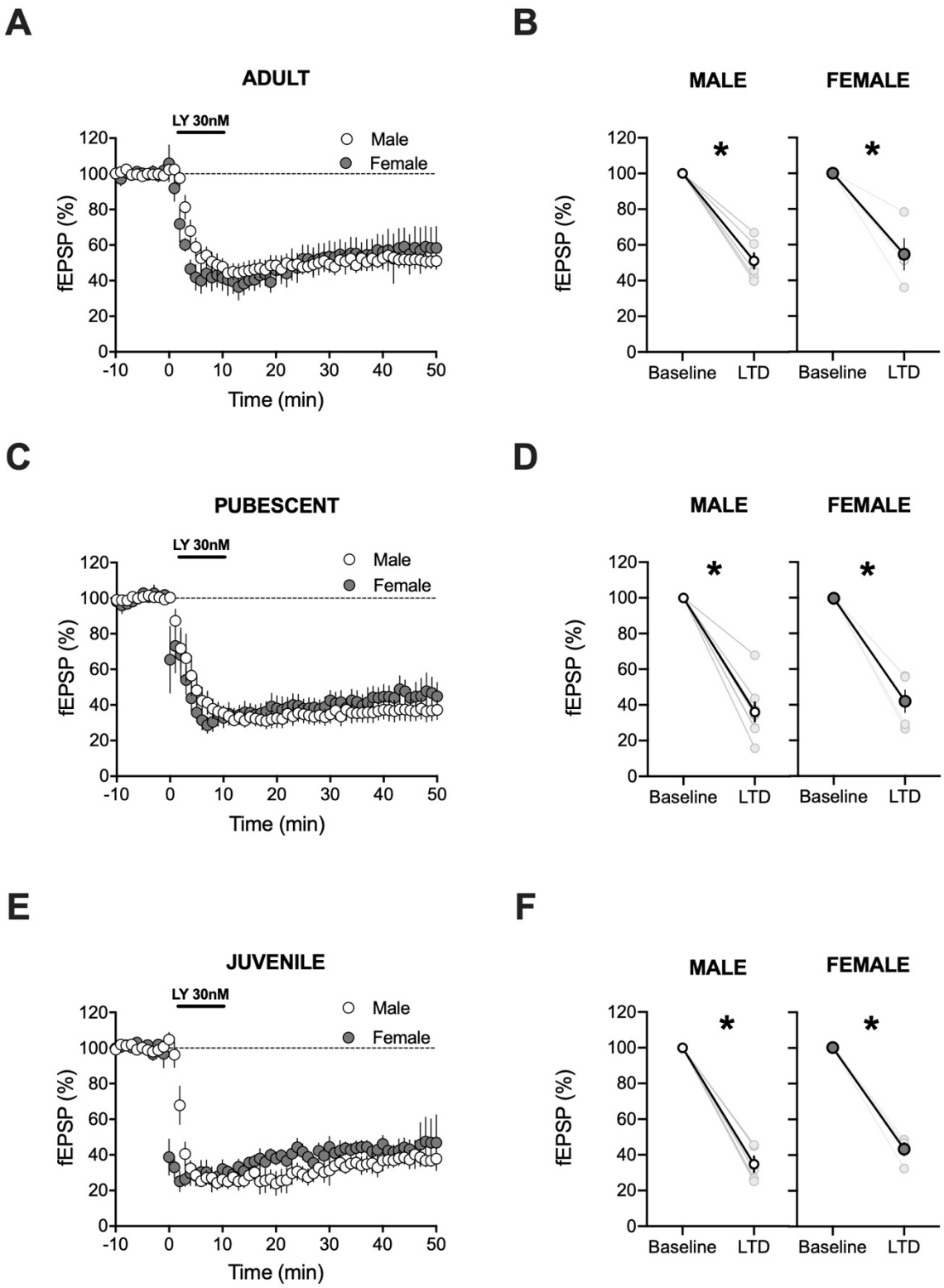
A
ADULT
LY 30nM
Male
Female
fEPSP (%)
Time (min)
B
MALE
FEMALE
fEPSP (%)
Baseline
LTD
C
PUBESCENT
D
E
JUVENILE
F

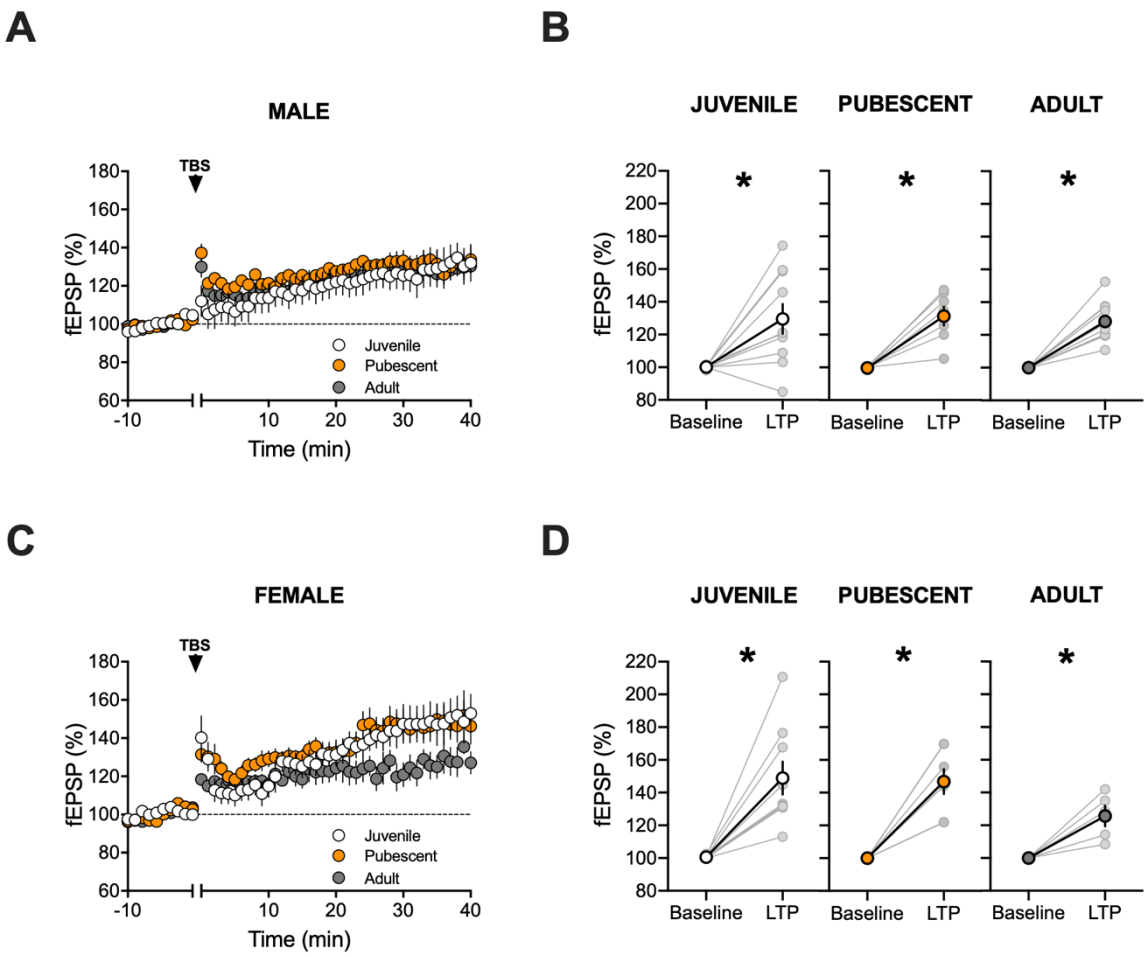
A
MALE
TBS
fEPSP (%)
Time (min)
Juvenile
Pubescent
Adult
B
JUVENILE
PUBESCENT
ADULT
fEPSP (%)
Baseline
LTP
C
FEMALE
TBS
fEPSP (%)
Time (min)
Juvenile
Pubescent
Adult
D
JUVENILE
PUBESCENT
ADULT
fEPSP (%)
Baseline
LTP

Tables

Table 1: Taqman probe and primers. Catalog numbers for the Taqman probe and primer sets from ThermoFisher Scientific (Waltham, MA, USA).

Gene	Cat. Number
CB1	1897316
CB2	1922303
mGluR5	1846135
TRPV1	1881063
DAGLα	1848623
DAGLβ	1898693
NAPE-PLD	1840797
MAGL	1709320
FAAH	1839106
ABHD6	1690662
CRIP1a	PN4351372
GAPDH	PN4351370

Table 2. eCB-LTD in the PFC data; comparisons by age
Values are mean ± SEM. F: Female, M: Male, J: Juvenile; P: Pubescent, A: Adult. Bold characters represent statistics with significant p values.

Test – Measure (unit)	**Condition**		**Value (mean, SEM, n)**	**Two tailed paired T-test**
eCB-LTD Normalized fEPSP 0-10min baseline vs 30-40min post-tetanus **(%)**	**M**	J	102,1 ± 3,069 N=10	P = 0,512
		P	75,91 ± 5,153 N=10	**P = 0,001**
		A	76,41 ± 2,741 N=19	**P < 0,0001**
	F	J	81,25 ± 3,263 N=14	**P < 0,0001**
		P	83,27 ± 3,609 N=16	**P = 0,0002**
		A	83,51 ± 3,603 N=8	**P = 0,0026**
				Ordinary one-way ANOVA Tukey multiple comparisons
eCB-LTD Normalized fEPSP 30-40min post-tetanus **(%)**	**M**	J	102,1 ± 3,069 N=10	**$F_{(2, 36)}$ = 15,43 ; P<0,0001 Juvenile vs Pubescent ; P<0,0001 Juvenile vs Adult; P=0,001**
		P	75,91 ± 5,153 N=10	
		A	76,41 ± 2,741 N=19	
	F	J	81,25 ± 3,263 N=14	$F_{(2, 32)}$ = 0,5402; P=0,5878
		P	83,27 ± 3,609 N=16	
		A	83,51 ± 3,603 N=8	

Table 3. eCB-LTD in the PFC data; comparisons by sex
Values are mean ± SEM. F: Female, M: Male, J: Juvenile; P: Pubescent, A: Adult. Bold characters represent statistics with significant p values.

Test – Measure (unit)	**Condition**		**Value (mean, SEM, n)**	**Two tailed unpaired T-test**
eCB-LTD Normalized fEPSP 30-40min post-tetanus **(%)**	**P**	M	75,91 ± 5,153 N=10	P = 0,3007
		F	83,27 ± 3,609 N=16	
	A	M	76,41 ± 2,741 N=19	P = 0,1546
		F	83,51 ± 3,603 N=8	

Table 4. eCB-LTD in the NAc data; comparisons by age
Values are mean ± SEM. F: Female, M: Male, J: Juvenile; P: Pubescent, A: Adult. Bold characters represent statistics with significant p values.

Test – Measure (unit)	**Condition**		**Value (mean, SEM, n)**	**Two tailed paired T-test**
eCB-LTD Normalized fEPSP 0-10min baseline vs 30-40min post-tetanus **(%)**	**M**	J	83.81 ± 3.826 N=14	**P = 0.002**
		P	83.75 ± 3.428 N=5	**P = 0.001**
		A	73.68 ± 3.605 N=5	**P < 0.0001**
	F	J	90.14 ± 2.544 N=5	**P = 0.014**
		P	84.17 ± 5.411 N=5	**P = 0.022**
		A	80.09 ± 8.451 N=5	**P = 0.046**

Table 5. mGlu2/3-LTD data, by age
Values are mean ± SEM. F: Female, M: Male, J: Juvenile; P: Pubescent, A: Adult. Bold characters represent statistics with significant p values.

Test – Measure (unit)	**Condition**		**Value (mean, SEM, n)**	**Two tailed paired T-test**
LY379268-LTD Normalized fEPSP 0-10min baseline vs 30-40min post-tetanus **(%)**	**M**	J	34,77 ± 4,410 N=5	**P = 0,0001**
		P	36,02 ± 5,429 N=8	**P = 0,0001**
		A	51 ± 4,395 N=6	**P = 0,0001**
	F	J	43,33 ± 3,698 N=4	**P = 0,0005**
		P	41,9 ± 3,609 N=5	**P = 0,0008**
		A	54,63 ± 8,768 N=4	**P = 0,0140**
				Ordinary one-way ANOVA Tukey multiple comparisons
LY379268-LTD Normalized fEPSP 30-40min post-tetanus **(%)**	**M**	J	34,77 ± 4,410 N=5	$F_{(2, 16)}$ = 3,014; P=0,0775
		P	36,02 ± 5,429 N=8	
		A	51 ± 4,395 N=6	
	F	J	43,33 ± 3,698 N=4	$F_{(2, 10)}$ = 1,088; P=0,3737
		P	41,9 ± 3,609 N=5	
		A	54,63 ± 8,768 N=4	

Table 6. mGlu2/3-LTD data, by sex
Values are mean ± SEM. F: Female, M: Male, J: Juvenile; P: Pubescent, A: Adult. Bold characters represent statistics with significant p values.

Test – Measure (unit)	**Condition**		**Value (mean, SEM, n)**	**Two tailed unpaired T-test**
LY379268-LTD Normalized fEPSP 30-40min post-tetanus **(%)**	**J**	M	34,77 ± 4,410 N=5	P = 0,1943
		F	43,33 ± 3,698 N=4	
	P	M	36,02 ± 5,429 N=8	P = 0,5032
		F	41,9 ± 3,609 N=5	
	A	M	51 ± 4,395 N=6	P = 0,6923
		F	54,63 ± 8,768 N=4	

Table 7. LTP-TBS data, by age

Values are mean ± SEM. F: Female, M: Male, J: Juvenile; P: Pubescent, A: Adult. Bold characters represent statistics with significant p values.

Test – Measure (unit)	**Condition**		**Value (mean, SEM, n)**	**Two tailed paired T-test**
LTP-TBS Normalized fEPSP 0-10min baseline vs 30-40min post-tetanus **(%)**	**M**	J	129,5 ± 9,073 N=10	**P = 0,0102**
		P	131,3 ± 5,748 N=7	**P = 0,0016**
		A	128,2 ± 3,487 N=11	**P = 0,0001**
	F	J	148,9 ± 10,13 N=9	**P = 0,0013**
		P	146,8 ± 7,542 N=7	**P = 0,0008**
		A	125,7 ± 6,286 N=5	**P = 0,015**
				Ordinary one-way ANOVA Tukey multiple comparisons
LTP-TBS Normalized fEPSP 30-40min post-tetanus **(%)**	**M**	J	129,5 ± 9,073 N=10	$F_{(2, 25)}$ = 0,048; P=0,9527
		P	131,3 ± 5,748 N=7	
		A	128,2 ± 3,487 N=11	
	F	J	148,9 ± 10,13 N=9	$F_{(2, 18)}$ = 1,631; P=0,2234
		P	146,8 ± 7,542 N=7	
		A	125,7 ± 6,286 N=5	

Table 8. LTP-TBS data, by sex
Values are mean ± SEM. F: Female, M: Male, J: Juvenile; P: Pubescent, A: Adult. Bold characters represent statistics with significant p values.

Test – Measure (unit)	Condition		Value (mean, SEM, n)	Two tailed unpaired T-test
LTP-TBS Normalized fEPSP 30-40min post-tetanus **(%)**	**J**		129,5 ± 9,073 N=10	P = 0,1704
		F	148,9 ± 10,13 N=9	
	P	M	131,3 ± 5,748 N=7	P = 0,1272
		F	146,8 ± 7,542 N=7	
	A	M	128,2 ± 3,487 N=11	P = 0,7077
		F	125,7 ± 6,286 N=5	

Table 9. Intrinsic properties data, by age
Values are mean ± SEM. F: Female, M: Male, J: Juvenile; P: Pubescent, A: Adult. Bold characters represent statistics with significant p values.

Test – Measure (unit)	Condition		Value	Ordinary one-way ANOVA Tukey multiple comparisons
Vm charges (mV)	**M**	J	N=16	$F_{(2, 30)}$ = 0,3808; P=0,6866
		P	N=9	
		A	N=8	
	F	J	N=9	$F_{(2, 30)}$ = 0,2674; P=0,7672
		P	N=6	
		A	N=7	
Number of spikes	**M**	J	N=16	$F_{(2, 36)}$ = 0,1771; P=0,8385
		P	N=9	
		A	N=8	
	F	J	N=9	$F_{(2, 36)}$ = 1,619; P=0,2122
		P	N=6	
		A	N=7	

Table 10. Intrinsic properties data, by age
Values are mean ± SEM. F: Female, M: Male, J: Juvenile; P: Pubescent, A: Adult. Bold characters represent statistics with significant p values.

Test – Measure (unit)	**Condition**		**Value**	**Ordinary one-way ANOVA Tukey multiple comparisons**
Resting membrane potential (mV)	**M**	J	-69,25 ± 1,010 N=16	$F_{(2, 31)}$ = 2,441; P=0,1037
		P	-70,53 ± 1,263 N=9	
		A	-73,21 ± 1,625 N=8	
	F	J	-69,81 ± 2,077 N=9	$F_{(2, 19)}$ = 1,330; P=0,2880
		P	-67,13 ± 0,9310 N=6	
		A	-71,68 ± 1,843 N=7	
Rheobase (pA)	**M**	J	111,4 ± 8,881 N=16	$F_{(2, 30)}$ = 0,2810; P=0,7570
		P	113,1 ± 19,95 N=9	
		A	125±14,94 N=8	
	F	J	134,4±1,752 N=9	$F_{(2, 18)}$ = 0,2178; P=0,8063
		P	144,4±23,45 N=6	
		A	128,8±19,83 N=7	

Table 11. Intrinsic properties data, by sex
Values are mean ± SEM. F: Female, M: Male, J: Juvenile; P: Pubescent, A: Adult. Bold characters represent statistics with significant p values.

Test – Measure (unit)	**Condition**		**Value**	**Two-way RM ANOVA; Sidak multiple comparisons**
Vm charges (mV)	**J**	Male	N=16	$F_{(10, 264)}$ = 0,09421; P=0,9999
		Female	N=9	
	P	Male	N=9	$F_{(10, 143)}$ = 0,1164; P=0,9996
		Female	N=6	
	A	Male	N=8	$F_{(10, 143)}$ = 0,3991; P=0,9453
		Female	N=7	
Number of spikes	**J**	Male	N=16	$F_{(12, 313)}$ = 0,1069; P>0,9999
		Female	N=9	
	P	Male	N=9	$F_{(12, 169)}$ = 0,2945; P=0,9896
		Female	N=6	
	A	Male	N=8	$F_{(12, 169)}$ = 0,1679; P=0,9993
		Female	N=7	

Table 12. Intrinsic properties data, by sex
Values are mean ± SEM. F: Female, M: Male, J: Juvenile; P: Pubescent, A: Adult. Bold characters represent statistics with significant p values.

Test – Measure (unit)	**Condition**		**Value**	**Two tailed unpaired T-test**
Resting membrane potential (mV)	**J**	M	-69,25 ± 1,010 N=16	P = 0,7871
		F	-69,81 ± 2,077 N=9	
	P	M	-70,53 ± 1,263 N=9	P = 0,0720
		F	-67,13 ± 0,9310 N=8	
	A	M	-73,21 ± 1,625 N=8	P = 0,5442
		F	-71,68 ± 1,843 N=7	
Rheobase (pA)	**J**	M	111,4 ± 8,881 N=16	P = 0,0933
		F	134,4±1,752 N=9	
	P	M	113,1 ± 19,95 N=9	P = 0,3279
		F	144,4±23,45 N=8	
	A	M	125±14,94 N=8	P = 0,8786
		F	128,8±19,83 N=7	

Table 13. Input-output data, by sex
Values are mean ± SEM. F: Female, M: Male, P: Pubescent, A: Adult. Bold characters represent statistics with significant p values.

Test – Measure (unit)	**Condition**		**Value**	**Two Way RM ANOVA; Sidak multiple comparisons**
input (µA)	**J**	M	N=9	$F_{(8, 168)}$ = 0,07051; P=0,9998
		F	N=12	
	P	M	N=12	$F_{(8, 204)}$ = 0,5453; P=0,8214
		F	N=13	
	A	M	N=7	$F_{(8, 189)}$ = 0,08236; P=0,9996
		F	N=16	

Table 14. Input-output data, by age
Values are mean ± SEM. F: Female, M: Male, P: Pubescent, A: Adult. Bold characters represent statistics with significant p values.

Test – Measure (unit)	**Condition**		**Value**	**Two Way RM ANOVA; Tukey multiple comparisons**
input (µA)	**M**	J	N=9	$F_{(16, 219)}$ = 01850; P=0,9998
		P	N=12	
		A	N=7	
	F	J	N=12	$F_{(16, 333)}$ = 0,1318; P>0,999
		P	N=13	
		A	N=16	

Table 15. Paired pulse ratio data, by sex
Values are mean ± SEM. F: Female, M: Male, J: Juvenile; P: Pubescent, A: Adult. Bold characters represent statistics with significant p values.

Test – Measure (unit)	**Condition**		**Value**	**Two Way RM A NOVA Sidak multiple comparisons**
Paired pulse ratio	**J**	M	N= 6 cells; 3 rats	$F_{(9, 80)}$ = 0,6689; P=0,7345
		F	N= 4 cells; 2 rats	
	P	M	N= 9 cells; 6 rats	$F_{(9, 130)}$ = 0,7029; P=0,7053
		F	N= 7 cells; 6 rats	
	A	M	N= 4 cells; 3 rats	$F_{(9, 98)}$ = 0,2945; P=0,9748
		F	N=8 cells; 7 rats	

Table 16. Paired pulse ratio data by age
Values are mean ± SEM. F: Female, M: Male, J: Juvenile; P: Pubescent, A: Adult. Bold characters represent statistics with significant p values.

Test – Measure (unit)	**Condition**		**Value**	**Two Way RM A NOVA Tukey multiple comparisons**
Paired pulse ratio	**M**	J	N= 6 cells; 3 rats	$F_{(18, 150)}$ = 0,5571; P=0,9246
		P	N= 4 cells; 2 rats	
		A	N=4 cells; 3 rats	
	F	J	N=4 cells; 2 rats	$F_{(18, 158)}$ = 0, 6779; P=0,8293
		P	N=7 cells; 5 rats	
		A	N= 8 cells; 5 rats	

Table 17. Pharmacology of eCB-LTD in the PFC data, in males
Values are mean ± SEM. F: Female, M: Male, P: Pubescent, A: Adult. Bold characters represent statistics with significant p values.

Test – Measure (unit)	**Condition**		**Value**	**Two tailed paired T-test**
eCB-LTD Normalized fEPSP 30-40min post-tetanus **(%)**	**SR 14176A**	P	98,92 ± 9,178 N=5	P = 0,9121
		A	105,8 ± 11,85 N=5	P = 0,6527
	AMG 9810	P	73,8 ± 8,158 N=5	**P = 0,0325**
		A	79,61 ± 3,39 N=11	**P = 0,0001**
	JZL 184	P	78,64 ± 3,842 N=4	**P = 0,0119**

Table 18. Pharmacology of eCB-LTD in the PFC data, in females
Values are mean ± SEM. F: Female, M: Male, J: Juvenile; P: Pubescent, A: Adult. Bold characters represent statistics with significant p values.

Test – Measure (unit)	**Condition**		**Value**	**Tow tailed paired T-test**
eCB-LTD Normalized fEPSP 30-40min post-tetanus **(%)**	**SR 14176A**	J	99,35 ± 3,956 N=5	P = 0,8783
		P	97,15 ± 5,174 N=9	P = 0,5965
		A	73,7 ± 8,178 N=6	**P = 0,0236**
	AMG 9810	J	98,17 ± 3,93 N=13	P = 0,6508
		P	75,44 ± 6,278 N=7	**P = 0,0079**
		A	106,8 ± 3,262 N=5	P = 0,1057

Table 19. Changes in mRNA levels of key components of the eCB system data, by age and sex

Values are mean ± SEM. F: Female, M: Male, J: Juvenile; P: Pubescent, A: Adult. Bold characters represent statistics with significant p values.

		J		P		A	
Targets	**Sex**	**n**	**p value**	**n**	**p value**	**n**	**p value**
CB1	F	8	0,999	8	**<0.0001**	8	**0,0002**
	M	8		7		8	
CB2	F	8	**0,0005**	8	**<0.0001**	8	0,5045
	M	8		8		8	
mGluR1	F	8	0,2747	8	0,5494	8	0,9768
	M	8		8		8	
mGluR5	F	8	**0,0006**	8	**<0.0001**	8	**<0.0001**
	M	8		8		8	
TRPV1	F	8	0,2580	8	**0,0032**	8	**<0.0001**
	M	8		8		8	
DAGLα	F	8	**0,0048**	8	0,1056	8	0,9868
	M	8		8		8	
DAGLβ	F	8	0,8287	8	>0.9999	8	0,7092
	M	8		8		8	
NAPE-PLD	F	8	**<0.0001**	8	**<0.0001**	8	**<0.0001**
	M	8		8		8	
MAGL	F	8	**<0.0001**	8	0,0866	8	**0,0073**
	M	8		8		8	
FAAH	F	8	**<0.0001**	8	**0,0006**	8	0,0940
	M	8		8		8	
ABHD6	F	8	**<0.0001**	8	0,3445	8	>0.9999
	M	8		8		8	
CRIP1a	F	8	**<0.0001**	8	0,8622	8	0,1951
	M	8		8		8	

Table 20. Effects of inhibitors of eCB catabolic enzymes on the induction of LTD in juvenile males, PFC data

Values are mean ± SEM. Bold characters represent statistics with significant p values.

Test – Measure (unit)	**Condition**	**Value**	**Mann-Whitney test**
eCB-LTD Normalized fEPSP 30-40min post-tetanus **(%)**	**JZL184**	78,64 ± 3,842 N=10	**P = 0,004**
	JZL184 + SR141716	98,92 ± 9,178 N=4	P = 0,111
	WWL70	85,00 ± 5,894 N=8	**P = 0,012**
	URB597	93,64 ± 3,350 N=9	P = 0,156